UNIVERSITY OF GEORGIA
Warnell School of Forestry & Natural Resources

Publication WSFNR-21-78A

December 2021

Tree Biomechanics: Basic Understandings Of Structure & Load

Dr. Kim D. Coder, Professor of Tree Biology & Health Care / University Hill Fellow
University of Georgia Warnell School of Forestry & Natural Resources

Trees are tall woody perennial plants with a porous and flexible sail, held aloft on a tapered mast with a stiff core covered by a reactive skin, and sitting upon and woven into a near-surface soil matrix. The three primary structural components of tree resistance to a chaotic and variable environment are its sail, height, and size. Figure 1. (Coder 2021a) This training manual will examine all three of these structural components and their interactions with wind loads.

A Full Sail

Understanding wind loads on trees is appreciating drag against, over and through tree crowns, both with and without leaves. Figure 2. Wind loads on trees with leaves greatly exceeds trees without leaves as wind velocity increases. How big is a tree's sail and how much wind does it catch? First, how large are the wind loads? The wind load on a tree per square foot of area rapidly accelerates as wind velocity increases. Figure 3. For every doubling of wind velocity, wind loads on tree surfaces increase by roughly four times (i.e. quadruples). Estimated wind pressures in pounds per square feet (lbs/ft^2) on tree frontal area can be calculated under standard conditions for various wind velocities in miles per hour (mph), allowing for recognition of load values on trees. (Coder 2021d) Figure 4.

The amount of load applied across the side face or frontal area of a tree crown, as well as through the crown volume, is not determined solely by the total amount of momentum present in wind. Depending upon tree structural density and its flexibility to fall back against the wind, some portion of wind load is applied to tree components, and some portion passes by. (Gardiner et al. 2016) The total force (F) applied to a tree sail by wind is: F = (0.5 X air density) X frontal area of tree toward wind X tree drag coefficient X wind speed squared modified by a Vogel number. (Gardiner et al. 2016; Mayhead 1973)

Frontal areas of trees appear as critical load variables in many tree failure formulae. (Peltola et al. 2000) Figure 5 shows relative frontal areas by standard crown shapes. In looking at a combined formula for tree stability (derived from Fournier et al. 2013; Jackson et al. 2019; Niez et al. 2019), increases in tree frontal area, drag coefficient, total height, crown mass and crown asymmetry are all changing over time at different rates, and all interact to cause tree failure from wind and gravity loads.

Facing The Wind

As wind speed increases, the frontal area of a tree and drag coefficient are reduced, while crown porosity increases. (Borisevich & Vikhrenko 2018; Gardiner et al. 2016; Kitagawa et al. 2015; Koizumi et al. 2016; Manickathan et al. 2018; Moore et al. 2018; Vollsinger et al. 2005) Figure 6 shows a simple structural model with load centers and significant tree measures. Foliage, twig, and branch reconfiguration and streamlining play important roles in tree wind loads. Figure 7 provides one means of estimating tree reconfiguration or reorientation back against the wind. As wind pressure increase, tree crowns reach maxiumu reconfiguration at wind speeds of approximately 55 mph or a frontal pressure of 8 pd/ft^2. (Coder 2021d) Wind forces are highly variable on porous crowned, flexible trees where frontal areas decline with increasing wind speed as branches and leaves streamline downwind.

Examples of crown reconfiguration include, a 45 mph wind reduced tree frontal area by ~43% compared with a tree standing in still air. (Rudnicki et.al 2004) Frontal area of trees were reduced in a 45 mph wind by 20% to 54% (Moore et al. 2018), with an average of 28%. (Vollsinger et al. 2005) Figure 8. Tree reconfiguration and reduction of crown frontal area was 20% for wind speeds less than 22 mph, and 60% for wind speeds more than 45 mph (Wu & Shao 2016). Arboricultural practices helped reduce frontal crown areas ~32% with intensive pruning, which was equivalent to a tree streamlining in a 40 mph wind. (Kitagawa et al. 2015) Remember across these tree studies, there is only a limited set of species, populations, crown forms, and wind environments examined.

Crown Density

Another component of tree frontal area blocking wind is associated with crown density. Visible crown porosity or openness shows how easily wind enters and passes through a tree crown. As wind load increases, crown frontal area decreases and crown porosity increases. (Gardiner et al. 2016) There are two measures of crown porosity in trees: optical porosity estimating crown density by a visual mix of open and closed spaces; and, aerodynamic porosity measured by how wind moves through the crown. (Gonzales et al. 2018) Figure 9 shows various levels of crown optical porosity or visual density, and wind flow through a tree crown termed aerodynamic porosity.

With increasing aerodynamic porosity up to 40%, air flow is moving around a tree crown, and wind loads increase. Above this critical level of aerodynamic porosity, wind flow bleeds through tree crowns and relative wind loads begin to fall quickly. (Manickathan et al. 2018) As wind speeds increase, frontal area of a tree and its drag coefficient change, and eventually aerodynamic porosity increases due to tree reconfiguration and streamlining. (Borisevich & Vikhrenko 2018; Gardiner et al. 2016; Koizumi et al. 2016; Manickathan et al. 2018; Mayhead 1973)

Wind Sieve

Comparing a visual assessment of crown density versus actual aerodynamic crown density or openness shows visual estimation of crown density or porosity underestimates actual wind load impacts through tree crowns. (Manickathan et al. 2018; Gonzales et al. 2018) Figure 10. Tree crown porosity measures and associated wind loads are important considerations for tree health care providers. Small, initial changes in crown density

by increasing porosity through crown thinning and pruning, might actually increase total wind loads on a tree as drag increases. Figure 11. More intensive crown thinning (>40% aerodynamic porosity) might significantly increase crown porosity and reduce tree wind loads. (Manickathan et al. 2018)

Drag Coefficient

Only a portion of energy in a wind stream is transferred to a tree. A ***drag coefficient*** represents the portion of wind momentum absorbed by a tree. (Gardiner et al. 2016) A drag coefficient is a measure of tree surface area or volume directly interacting with or blocking wind. Interestingly, drag coefficients determined under open landscape conditions with dynamic wind loads and full-sized trees are significantly greater than drag coefficients measured in indoor wind tunnel tests or generated by computer imaging. (Koizumi et al. 2016)

Wind load on a tree is always a combination of tree frontal area toward the wind, wind speed, and drag coefficient. Drag coefficients in trees decrease with increasing wind speed. (Gardiner et al. 2016; Mayhead 1973) Trees streamline, reorient, or reconfigure in either a plastic (flexing) or brittle (breaking) way. As tree parts fall back against increasing wind, frontal areas change and drag coefficients decline until a tree cannot reconfigure anymore without breaking. As wind speeds increase to greater than ~65 mph, and trees complete all plastic reconfiguration possible, drag coefficients become nearly constant. (Mayhead 1973)

Different Coefficients

Drag coefficients can vary by season, species, and measurement method. Leaves being off or on a tree make a great difference. Because tree frontal areas reconfigure (becomes smaller) with increasing wind speed, drag coefficients change. Drag coefficients should always be identified with the wind speed when they were measured. Examining a number of tree drag coefficients from recent research papers showed the range, variation, and values of tree drag coefficients. Figure 12. Average tree drag coefficients were found to be: 0.55 (static measure, n=15 since 2014); 0.54 (at 22 mph, n=8 since 2015); and, 0.34 (at 45 mph, n=16 since 2005).

For all tree drag coefficients, average leaves-on was 0.72, and average leaves-off was 0.41, suggesting leaves account for an average of 0.31 of a tree drag coefficient value. Large variations are present for tree drag coefficients at wind speeds below 16 mph due to swaying and associated damping of stem and branches. As wind speeds increase, less swaying is present and drag coefficients approach a constant value. (Koizumi et al. 2016; Rudnicki et al. 2004)

Vogel Corrections

The final modification needed for understanding tree sail resisting wind loads is wind speed. Wind loads in trees are not proportional to simply wind speed squared as with static objects. (Moore et al. 2018) The squared value of wind speed must be reduced because trees are not static solid objects like a building or a car, but actively reorient and streamline – falling back against the wind. Assessing reorientation of trees through wind speed requires use of a ***Vogel number***. A Vogel number or exponent (V) is used to reduce the square exponent of wind velocity (wind speed $^{2-V}$) , and represents decay in the drag coefficient as a tree reorientates and streamlines. (Gardiner et al. 2016; Manickathan et al. 2018)

The theoretical Vogel exponent value in trees is approximately -0.66, decreasing the wind speed squared exponent from 2.0 to 1.34 for calculating wind loads (wind speed $^{2 - 0.66}$ = wind speed $^{1.34}$). Examining multiple Vogel numbers from tree research demonstrate how changes in wind speed inputs are applied to wind loads. Figure 13. An all-species average Vogel exponent was found to be -0.51, yielding a wind speed exponent of 1.49 (n=15, since 2008). Average Vogel numbers of all species with leaves-on were -0.39 (n=5) and with leaves-off were -0.28 (n=4), suggesting leaves accounted for -0.11 of the Vogel exponent, decreasing wind speed exponents for trees with leaves.

Lopsided

Throughout these calculations of wind loads, a balanced sail on top of a straight tapered mast is assumed. Few trees, or large branches, are perfectly balanced and symmetrical. Lopsided or asymmetrical crowns in wind can generate torsion or twist along tree structures. Tree tissues under torsion take less force to break. Asymmetrical wind loads on tree crowns and individual branches mean less total wind load causes tree failure. Bending and twisting conspire to break trees in unexpected ways and at unexpected load levels. Alternatively, trees challenged by torsional loading can generate added resistance to twisting and bending over time seen sometines as spiral grain xylem.

Sailing Away

The sail of a tree, successfully held aloft while resisting dynamic wind loads, is a major mechanical investment for a tree over its life. A tree surviving and thriving depends upon optimizing both biology and structure. With applied wind loads in trees being proportional to combined frontal area, wind speed, and height, it is clear reducing tree height, extent and reach of large branches, and frontal area of tree through pruning can reduce wind loads. (Stubbs et al. 2019) Tree health care providers can help better manage tree mechanics through thoughtful crown reduction and thinning, as well as pruning for crown and branch symmetry.

Tree Height Plight

One of the easiest factors to visualize leading to tree failure involves tree height above its surroundings and its crown mass concentrated at the top. The greater tree height, the higher center of wind load on its crown. Key features of many tree safety and failure formulae are tree total height, tree functional height (center of wind load height), crown mass, and height-associated stem taper or slenderness. Figure 14. (Coder 2021b)

Taller vs. Shorter

Trees gather light resources with increasing height growth. But safety from wind loads come from both a shorter functional tree height [tree height - (live crown height X 0.4)] associated with a lower center of wind load, and from a decreased total tree height. (Dellwik et al. 2019; Fournier et al. 2013; Niez et al. 2019) Figure 15. Stem leans and other displacements will initiate quick tree reactions to regain vertical growth for light harvesting. This tree posture control is focused upon extending tree height and branch length, which continually shifts structural loads. Attributes critical to tree structural geometry (both in success and failure) include height, crown mass and its position along the stem, and stem taper. (Fournier et al. 2013)

Tree stability factors under wind loads are dominated by height to the fourth power [(height^4) / (0.5 X diameter)]. (Niklas & Spatz 2012) Because applied bending loads in trees are proportional to height, a taller tree with a more extensive crown higher along its stem has both greater drag and applied bending loads than a shorter smaller tree. (MacFarlane & Kane 2017; Stubbs et al. 2019) The center of wind load in a tree crown, or the functional tree height, is concentrated around 60% of crown height. (Dellwik et al. 2019) Tree failure risks decrease with smaller crown mass, greater live crown ratio, less total height, and less functional height. (Peterson et al. 2019; Urata et al. 2012) Figure 16 expands and refines an earlier tree structural figure to show height associated measures in a tree.

Height Resources

When trees are continually challenged by wind bending and flexing (swaying & damping), trees will reallocate growth resources to generate more rigidity and less height growth. (Niez et al. 2019; Niklas & Spatz 2012) Wind loads stimulate shorter height growth, more diameter growth, and reallocation of growth resources to the root system. (Gardiner et al. 2016; Telewski & Moore 2016; Wu et al. 2016) As height growth is reduced under wind loads, more food is made available for stem and roots, and reduced branch mass. (Nicoll et al. 2019) In one example of internal reallocation of growth resources, wind load stimulation of small container trees decreased height by ~5%, increased diameter by ~30%, and increased cross-sectional area by 189%. In this case with small container trees, safety increased by +134% due to wind stimulation. (Niez et al. 2019) Figure 17 demonstrates as more wind challanges to trees are applied, trees generate less height growth. (Nicoll et al. 2019)

Open Growing

Open grown trees challenged by wind from all sides tend to be shorter, have greater stem taper especially near the base, and have a lower functional tree height. For stability, open grown trees generate greater rigidity in the stem and greater elasticity within the periphery of their crowns. (Jelonek et al. 2019) Across their long lives, trees experience increasing applied wind loads due to extension of height, expansion of crown reach and extent, increased diameter growth, and changing height / diameter ratios. These changes increase vulnerability of taller, older, and bigger trees to damage. (Gardiner et al. 2016; Niklas 2007; Niklas & Spatz 2012; Paz et al. 2018)

Trees with smaller or more flattened crowns, large live crown ratios, greater diameter, and shorter height are more stable under wind loads. (MacFarlane & Kane 2017; Peltola 2006; Peterson et al. 2019; ver Planck & MacFarlane 2019) Trees with wide or broad crowns presenting large frontal areas to wind loads showed only slightly more damage than trees with more narrow crowns (with the same height and live crown ratios). (Peterson et al. 2019) Figure 18 semonstrates as live crown ratios increase, on open grown mature trees, the wind speed leading to failure increases. (Urata et al. 2012) Greater live cown ratios are sustainable over greater wind loads. But, tree height (both actual height and functional height) remains a dominant feature responsible for tree stability or failure under applied wind loads.

Twist Preference

Branches are designed to be flexible and breakable. (Lopez et al. 2011) They move side-to-side, and up-and-down in a figure-8 motion with large movements side-to-side. Stems and branches twist 1.5 times more,

and preferably to, bending. (Niklas & Spatz 2012) Examining trees which were wind-thrown, large branches generated asymmetrical loads across crowns causing crown twist or torque. (ver Planck & MacFarlane 2019) Trees can be effective at resisting pure bending loads, but are more susceptible to failure when bending loads are combined with shear or torque. (Stubbs et al. 2019)

Stem and branch flexibility under bending changes as torque is applied causing tissues to become stiffer. Torsion loads reduce stem and branch flexibility, significantly lowering bending loads needed for failure. (Avalos & Sanchez 2014) Figure 19. In addition, as torsion increases, shear strength of the green tissue can be exceeded, resulting in a longitudinal split. (Wu & Shao 2016)

Torsion Loads

Torsion (twisting) failures increase with tree height, accentuated by asymmetrical crown loads especially along stem and big branches. (Virot et al. 2016) Increased height, large codominant branches, forks, and lopsided crowns all lead to increased bending and twisting loads. The maximum stress and strain along a stem is found near the base of the live crown where large branches are connected. (Lopez et al. 2011) It is tree height and not crown width, coupled with any uneven application of wind loads across lopsided crowns and large branches, that are the primary drivers of failure in trees. Asymmetrically applied loads can be partially managed with arboricultural practices.

There is a mechanical tuning within tree tissues between bending and torsion strains. Trees balance bending and torsion failure through growth to assure neither one is more likely to occur. (Skatter & Kucera 2000) Neglecting torsion on branches and stems, underestimates the risk of failure, even though torsion is a small component of wind load resistance compared to bending. (Avalos & Sanchez 2014) Torsion significantly decreases bending load resistance in trees and should not be ignored. (Skatter & Kucera 2000)

Crown Mass

Another important mechanical issue found in tree failure is a tall stem holding a heavy crown into the wind. (ver Planck & MacFarlane 2019) Most of above-ground mass in a tree is held in branches, not the stem. (James 2014) Branch and foliage mass contribute about 60% of crown mass. (Rudnicki et al. 2004; Vollsinger et al. 2005) Large crowns transfer large loads to the stem base and roots in the wind, potentially leading to increased damage. (Gardiner et al. 2019; Garms & Dean 2019; Paz et al. 2018) A large crown mass poses a higher failure risk by itself, with the amount of branch mass more critical than the total mass of a tree. (ver Planck & MacFarlane 2019)

Tree crown mass also adds to drag forces, reducing the total additional load needed to break a tree. (Dupont et al. 2015) Tree failure was found to depend both upon large branches generating asymmetrical loads across a crown (crown twist / torque), and upon massive crowns in general. (Telewski & Moore 2016; ver Planck & MacFarlane 2019) Because most of the drag in trees occurs near the ends of branches with leaves, shortening (abridging) large branches – not removing them, can decrease crown mass and potential damage. (Kane 2018; Rodriguez et al. 2008)

Risk Ratios

Large crown mass to stem mass ratios tend to be good predictors of tree failure risks. (Gardiner et al. 2019; Urata et al. 2012) In one study, when crown mass exceeded 43% of above-ground tree mass, tree failure probability exceeded 50%. (ver Planck & MacFarlane 2019) Figure 20. As shown previously, increased crown length to tree height ratios (i.e. increased live crown ratios) decreased wind damage risks due to lowered wind load center height (Gardiner et al. 2019; Peterson et al. 2019; Urata et al. 2012) Keeping lower branches on stems below the most flexible portion of a stem helps absorb and damp wind loads.

In a simple tree functional height- or length-based crown and branch treatment example, Figure 21 demonstrates how crown raising or branch over-cleaning or lion's tailing, can significantly increase potential loads on trees and branches. Figure 22 shows how crown reduction or branch abridging can decrease potential loads on trees and branches. Minimize crown raising treatments and utilize crown reduction treatments to reduce wind loads and minimize tree failure risks.

Slender Stems

Height / diameter relationships (taper) change with wind load challenges, causing trees to become more tapered. (Telewski & Moore 2016) Resistance to tree failure is associated with greater stem taper (diameter^2 : tree height) or less slenderness, and decreased height (Kabir et al. 2018; Moore 2000; Paz et al. 2018; Peltola et al. 2000) Active tree management, such as height reduction and intensive crown reduction and thinning, can significantly reduce applied wind loads and associated tree failure risks. (Koizumi et al. 2016)

Tree development of decreased diameter to height ratios (less taper or more slender) can be caused by carbohydrate starvation from lack of light. (MacFarlane & Kane 2017) Trees in shade or understories, or trees forced to re-form crowns after damage, would be most susceptible to failure from both torsion and bending loads due to less taper. As trees grow in height without increasing stiffness and radial growth, self-weight eventually causes bending which cannot be overcome and corrected. (Moulia et al. 2019)

Height-Diameter Impacts

Tree height and branch length generate long lever arms to which wind and gravity loads are applied, and to which trees must continually adjust. Tree safety in wind is increased with both stem diameter growth and decreased center of wind load height [(diameter)^3 / (tree height X frontal area)]. (Fournier et al. 2013; Hale et al. 2012; Niez et al. 2019) The tree height to diameter ratio (taper) minimizing wind damage is around a value of 66 and below. (Moore & Lin 2019)

Another tree form formula (derived from Fournier et al. 2013) uses increasing diameter [+ (tree diameter)$^{2.5}$] and decreasing height and mass [- (tree height) $^{2.25}$ X (above ground biomass)] as variables for tree mechanical success. All these observations show less stem diameter growth coupled with greater height growth under the same wind loads, eventually lead to catastrophic tree failure. Note that total height does remain more critical to tree damage risks than taper or slenderness alone. (ver Planck & MacFarlane 2019)

Being Tall & Top-Heavy

In examining what causes trees to fail, variables such as tree height, stem lean, stem weight, stem taper, crown weight, and crown height along a stem were all found to be important at some level. But, tree height and crown mass were found to be key measures of tree stability or failure. (Fournier et al. 2013; Jelonek et al. 2019) Arborists can reduce risks of tree failure through thoughtfully applied tree height reduction and crown mass control with symmetry corrections, while minimizing crown raising treatments.

Questions of Diameter

Another set of structural attributes which help support trees involve thickness or diameter of the stem, branches and structural roots. Tree diameter growth generates additional stiffness for resisting wind and gravity loads. Key features of tree stability then include stem and root diameters, and stiffness of stem and root base area. These features are included in a number of tree failure formulae. Figure 23. (Coder 2021c)

Changing Growth

Corrections in response to gravity and wind are part of long-term mechanical stability in trees, which is driven by increases in diameter to equalize structural loads. (Jelonek et al. 2019) The outer-most radial cell layers of xylem increase diameter, generating forces which resist and correct mechanical load imbalances. (Thibaut 2019) The environment applies wind and gravity loads, and trees in response must manage height and diameters to remain erect. Both diameter growth and height-to-diameter ratios are important biomechanical attributes under active control of a tree. (Niklas & Spatz 2012) Figure 24 shows how changes in taper (height to diameter ratios) impact tree failure. Large stem tapers hold against more wind loads before failure when compared with narrow or slender stems.

Trees experience increasing wind loads over their life due to expansion of height, increases in crown reach and extent, and changing height-to-diameter ratios. (Gardiner et al. 2016) Trees will generate less height growth, more root biomass, and greater diameter growth in response to wind loads. (Wu et al. 2016) In one study, trees exposed to bending loads increased diameter growth by >80% in response to wind. (Bonnesoeur et al. 2016) Trees which move in wind have greater stem and root base area diameter growth than trees prevented from moving. (Nicoll et al. 2019) Figure 25.

Height & Diameter Balance

There is always a structural trade-off between the diameter of stem and branches, and their height or length. As diameter increases, stem and branch stability and sway damping are improved for a given load environment. Simultaneously, as stem height or branch length increase, there are greater bending loads, increased drag coefficients from less reorientation, and more risk of failure. (Butler et al. 2012; MacFarlane & Kane 2017) Trees must continually reconfigure and reinforce their structure to resist both external loads and internal mechanical responses, which requires significant growth adjustment times.

Stems and branches develop greater mechanical resistance in their base with increased wood density, stiffness, and diameter growth, and less mechanical resistance at their tips, which provide flexibility with self-support.

(Ozden & Ennos 2018) In short, peripheral flexibility and basal stiffness generate a greater chance of long-term survivability in trees. (Niez et al. 2019)

Stiff vs. Flexible

There have been many studies examining the importance of diameter measures in tree stability. Each study is unique, examining different tree species of different sizes and ages, at various measurement locations within trees, and under varying wind load environments. Some single studies reach multiple descriptions of tree success and failure. Select tree diameter importance findings are given below:

– Tree cross-sectional area ($0.79 \times D^2$) at 10 feet above the ground was found to be the best predictor of stem breaking force. (Garms & Dean 2019)

– Tree stability is proportional to four times stem and branch cross-sectional area ($12.6 \times D^2$) increases in small container trees. (based upon the Fournier formula – Niez et al. 2019)

– Stem failure depends upon stem diameter squared times stem height ($D^2 \times$ height), representing 94% of tree failure variation. (Fournier et al. 2013; Gardiner et al. 2016; Hale et al. 2012; MacFarlane & Kane 2017; Moore 2000; Peltola et al. 2000)

– Tree stability was proportional to stem diameter growth ($D^{2.5}$) shifting between stiffness and flexibility along a stem or branch length. (derived from Fournier et al. 2013)

– Stem breakage depends upon diameter cubed (D^3), representing 96% of tree failure variation. (Fournier et al. 2013; Gardiner et al. 2016; Hale et al. 2012; MacFarlane & Kane 2017; Peltola et al. 2000)

– Bending resistance from both increased diameter growth and wood characteristic changes were 3.5 times greater in the bottom 10% of a stem or branch than anywhere else. (Sagi et al. 2019)

– Tree stiffness near the stem base was proportional to its diameter to the fourth power (D^4) and was the strongest determinant of stem safety. (Butler et al. 2012; Gardiner et al. 2016; Niklas & Spatz 2012)

Trees need to be both flexible and rigid at the same time to resist static (self-weighted) and dynamic (wind) forces. (Gardiner et al. 2016) With increasing height, tree tissues are less stiff near the tip of a tapered stem. (Dargahi et al. 2019) As suggested by the different diameter importance findings given above, trees continually modify their wind resistance along their height, generating stiffness near the stem base, and flexibility near the stem top. In between stem base and tree top is a transition zone between stiff and flexible which is actively shifted upward over time. (Koizumi et al. 2007). Figure 26.

Reallocating Resistance

Applied wind loads have great impact on stem and root diameter growth, especially in tree parts with the highest mechanical stress and strain. (Gardiner et al. 2019) Trees must reallocate growth resources to the stem base and structural root plate to remain stable. With wind, trees shift growth resources to more root biomass, greater stem base and root base diameter growth, increased stem taper, larger root-to-shoot ratios, increased root plate diameter, and altered xylem cell walls. (Gardiner et al. 2016; Gardiner et al. 2019; Nicoll et al. 2019; Telewski & Moore 2016; Wu et al. 2016)

Root Diameter

Bending and rotation at the tree base are counter-balanced by the root — soil system. (Niklas 2007) As wind intensity increases, vibrational impacts from tree top to rigid stem base and roots increase, loosening anchorage and increasing potential damage unless corrected by additional growth. (Dupont et al. 2018; Paz et al. 2018; ver Planck & MacFarlane 2019) Wind and gravity loads generate a "load wheel" rolling a tree out of the ground, to which a tree must generate and sustain resistance. (Coder 2010; Coder 2018) Figure 27.

Tree stability depends upon increasing stem base and basal root diameters, and root plate size and mass. (Gardiner et al. 2016) In addition, wind loads and associated sway applied from one direction increases elliptical cross-sectional root shapes near the stem base, and generates greater diameter growth in structural roots along the load axis. (Nicoll et al. 2019; Telewski & Moore 2016) Figure 28 shows the differences between maximum stress levels in three tree stem cross-sectional shapes. Eccentric growth forms help resist bending loads and minimzie stress.

Figure 29 shows cross-section shapes of structural roots around a tree's base generated to resist induced wind loads. Large roots near the stem base can be reinforced to resist bending and hinging by generating eccentric cross-sectional shapes like ovals, T-beams or I-beams in response to bending and twist. (Gardiner et al. 2016; Telewski & Moore 2016) Figure 30.

Root Plate & ZRT

Key components of tree root base resistance to failure includes a narrow compression ring (zone of rapid taper = ZRT) within a much broader rigid root plate area. Figure 31. The mass of large diameter structural roots at a tree's base, some with eccentric cross-section shapes, provide support, stiffness and resistance to failure. A generalized root plate diameter size in non-constraining soil conditions can be calculated by using tree stem diameter (DBH_{inches}) times 0.9, yielding root plate diameter in feet. (Coder 2018)

Within ~3.5 feet (the zone of rapid taper or ZRT area) of a tree base and within its root plate area, roots greatly increase diameter growth and basal taper, and associated resistance to compression, flexing, and torsion (twist). (Dorval et al. 2016; Stubbs et al. 2019) Root stiffness is greater close to the stem base and reflects both diameter and root growth geometry changes. (Sagi et al. 2019) This zone of rapid taper (ZRT) resists root bending, hinging or folding downward on the leeward side of any wind load. A generalized ZRT diameter size in non-constrained soil conditions can be calculated by tree diameter (DBH_{inches}) times 0.3, yielding ZRT diameter in feet. (Coder 2018) Figure 32.

Root Constraints

Risks of tree failure increase with restriction of structural rooting space. Some causes of constrained structural rooting space include: hardscape and infrastructure installation and presence; soil compaction, aeration and drainage issues; and/or mechanical issues of impervious layers below ground – all leading to much shallower but wider ZRTs and root plates. Under these constraints, even greater root cross-section shape changes can be generated (like stem base – root buttresses), and accelerated diameter growth. (Coder 2010; Coder 2018; Gardiner et al. 2016)

Root Growth & Form

Leeward root loads are dissipated by compression into soil close to the stem base (the ZRT), while windward roots of the root plate area are pulled in tension, sometimes out of the ground. (Coder 2010; Coder 2018; Watson 2000) Figure 33. Windward roots make 2-3 times the structural contribution to root and tree anchorage as do leeward roots. (Watson 2000) Root systems can be asymmetrical in distribution, with most roots growing toward the maximum load direction (Coder 2010; Coder 2018; Niklas & Spatz 2012), but with greater structural root mass developed on the leeward side where larger diameter roots generate increased stiffness. (Dorval et al. 2016; Telewski & Moore 2016)

To summarize tree root base issues: keep-off the root plate area with no compacting events, no trenching, and no root base / stem base injury; carefully apply treatments which do not shift functional balance between shoot and root growth; and, develop healthy soil and sites with few constraints to root health and growth.

Diameter for Success

Trees generate diameter growth preferentially in areas where stress and strain are greatest. Over time, stem diameters and root plate diameters continue to increase resistance to increasing loads, although at different rates. Figure 34. Because of this difference in diameter growth change over time, young trees tend to break, and old trees tend to uproot. Load challenges to stem and root base diameter growth generate unique structural components which must be conserved and protected from damage. Tree health care providers, tree risk managers, and arborists need to continually explore how trees remain upright in a changing environment which is trying to knock them down.

Conclusions

Because there are many papers and books examining how trees stand against wind over many years, this short review just highlights some of the issues. Tree structure must continue to change as it is challenged by the environment. Tree structure must also continue to change as its reactive skin of living tissues expand to colonize, collect, and hold resource containing volumes. The shed core skeleton of a tree represents only past load environments the tree has resisted. Structural success or failure of trees rest on their continuing correct adjustments to environmental constraints, growth opportunities, and human manipulations or injuries.

SELECTED LITERATURE

Angelou, N., E. Dellwik, & J. Mann. 2019. Wind load estimation on an open-grown European oak tree. Forestry 92:381-392.

Avalos, J. & A. Sanchez. 2014. Evaluation of failure criteria in branch members under torsion and bending moment. Arboriculture and Urban Forestry 40(1):36-45.

Bonnesocur, V., T. Constant, B. Moulia, M. Fournier. 2016. Forest trees filter chronic wind-signals to acclimate to high winds. New Phytologist 210:850-860.

Borisevich, S.A. & V.S. Vikhrenko. 2018. Evaluation of the drag coefficients of tree crowns by numerical modeling of their free fall. Agricultural and Forest Meteorology 256/257:346-352.

Butler, D.W., S.M. Gleason, I. Davidson, Y. Onoda, M. Westoby. 2012. Safety and streamlining of woody shoots in wind: An empirical study across 39 species in tropical Australia. New Phytologist 193:137-149.

Chiatante, D., S.G. Scippa, A. DiIorio, & M. Sarnataro. 2003. The influence of steep slopes on root system development. Journal of Plant Growth Regulation 21:247-260.

Coder, K.D. 2010. Tree anchorage: Root plate resistance to failure. Arborist News 19(3):52-56.

Coder, K.D. 2018. Tree Anchorage & Root Strength Manual. University of Georgia, Warnell School of Forestry & Natural Resources outreach publication WSFNR-18-37. Pp.69.

Coder, K.D. 2021a. Resisting the wind: Tree biomechanics basics, part 1. Arborist News 30(2):32-37.

Coder, K.D. 2021b. The plight of height and top-heavy: Tree biomechanics basics, part2. Arborist News 30(3):28-32.

Coder, K.D. 2021c. The meaning of diameter: Tree biomechanics basics, part 3. Arborist News 30(4):26-32.

Coder, K.D. 2021d. Trees and storm wind loads. University of Georgia, Warnell School of Forestry & Natural Resources outreach publication WSFNR-21-55C. Pp.47.

Danjon, F., T. Fourcaud, & D. Bert. 2005. Root architecture and wind-firmness of mature *Pinus pinaster*. New Phytologist 168:387-400.

Dargahi, M., T. Newson, & J. Moore. 2019. Buckling behavior of trees under self-weight loading. Forestry 92:393-405.

Dellwik, E., M.P. van der Laan, N. Angelou, J. Mann, A. Sogachev. 2019. Observed and modeled near-wake flow behind a solitary tree. Agricultural and Forest Meteorology 265:78-87.

DiIorio, A., B. Lasserre, G.S. Scippa, & D. Chiatante. 2005. Root system architecture of *Quercus pubescens* trees growing on different sloping conditions. Annals of Botany 95:351-361.

Dorval, A.D., C. Meredieu, F. Danjon. 2016. Anchorage failure of young trees in sandy soils is prevented by a rigid central part of the root system with various designs. Annals of Botany 118:747-762.

Dupont, S., D. Pivato, Y. Brunet. 2015. Wind damage propagation in forests. Agricultural and Forest Meteorology 214-215:243-251.

Dupont, S., P. Defossez, J-M. Bonnefond, M.R. Irvine, D. Garrigou. 2018. How stand tree motion impacts wind dynamics during windstorms. Agricultural and Forest Meteorology 262:42-58.

Fournier, M., J. Dlouha, G. Jaouen, T. Almeras. 2013. Integrative biomechanics for tree ecology: Beyond wood density and strength. Journal of Experimental Botany 64(15):4793-4815.

Gardiner, B., A. Achim, B. Nicoll, & J-C. Ruel. 2019. Understanding the interactions between wind and trees: An introduction to the IUFRO 8th wind and trees conference (2017). Forestry 92:375-380.

Gardiner, B., P. Berry, & B. Moulia. 2016. Review: Wind impacts on plant growth, mechanics and damage. Plant Science 245:94-118.

Garms, C. & T.J. Dean. 2019. Relative resistance to breaking of *Pinus taeda* and *Pinus palustris*. 2019. Forestry 92:417-424.

Gonzales, H.B., M.E. Casada, L.J. Hagen, J. Tatarko, R.G. Maghirang, C.J. Barden. 2018. Porosity and drag determination of a single-row vegetation barrier (*Maclura pomifera*). Transactions of the ASABE (American Society of Agricultural and Biological Engineers) 61(2):641-652.

Hale, S.E., B.A. Gardiner, A.Wellpott, B.C. Nicoll, A. Achim. 2012. Wind loading of trees: Influence of tree size and competition. European Journal of Forest Research 131:203-217.

Jackson, T., A. Shenkin, J. Moore, A. Bunce, T. van Emmerik, B. Kane, D. Burcham, K. James, J. Selker, K. Calders, N. Origo, M. Disney, A. Burt, P. Wilkes, P. Raumonen, J.G.deT. Menaca, A Lau, M. Herold, R.C. Goodman, T. Fourcaud, Y. Malhi. 2019. An architectural understanding of natural sway frequencies in trees. Journal of the Royal Society Interface 16:20190116.

James, K.R. 2014. A study of branch dynamics on an open-grown tree. Arboriculture & Urban Forestry 40(3):125-134.

Jelonek, T., A. Tomczak, Z. Karaszewski, M. Jakubowski, M. Arasimowicz-Jelonek, W. Grzywinski, J. Kopaczyk, K. Klimek. 2019. The biomechanical formation of trees. Drewno 62:5-22.

Kabir, E., S. Guikema, B. Kane. 2018. Statistical modeling of tree failures during storms. Reliability Engineering and System Safety 177:68-79.

Kane, B. 2018. The effect of simulated trunk splits, pruning, and cabling on sways of *Quercus rubra* L. Trees: Structure and Function 32:985-1000.

Kitagawa, K., S. Iwama, S. Fukui, Y. Sunaoka, H. Yazawa, A. Usami, M. Naramoto, T. Uchida, S. Saito, H. Mizunaga. 2015. Effects of components of the leaf area distribution on drag relations for *Cryptomeria japonica* and *Chamaecyparis obtusa*. European Journal of Forest Research 134:403-414.

Koizumi, A., M. Shimizu, Y. Sasaki, T. Hiral. 2016. In situ drag coefficient measurements for rooftop trees. Journal of Wood Science 62:363-369.

Koizumi, A., N. Oonuma, Y. Sasaki, & K. Takahashi. 2007. Difference in uprooting resistance among coniferous species planted in soils of volcanic origin. Journal of Forest Research 12:237-242.

Lopez, D., S. Michelin, E. de Langre. 2011. Flow-induced pruning of branched systems and brittle reconfiguration. Journal of Theoretical Biology 284:117-124.

Lundstrom, T., T. Jonas, V. Stockli, & W. Ammann. 2007. Anchorage of mature conifers: Resistive turning moment, root-soil plate geometry and root growth orientation. Tree Physiology 27:1217-1227.

MacFarlane, D.W. & B. Kane. 2017. Neighbor effects on tree architecture: Functional trade-offs balancing crown competitiveness with wind resistance. Functional Ecology 31:1624-1636.

Manickathan, L., T. Defraeye, J. Allegrini, D. Derome. 2018. Comparative study of flow field and drag coefficient of model and small natural trees in a wind tunnel. Urban Forestry and Urban Greening 35:230-239.

Mayhead, G.J. 1973. Some drag coefficients for British forest trees derived from wind tunnel studies. Agricultural Meteorology 12:123-130.

Moore, J. & Y. Lin. 2019. Determining the extent and drivers of attrition losses from wind using long-term datasets and machine learning techniques. Forestry 92:425-435.

Moore, J.R. 2000. Differences in maximum resistive bending moments of *Pinus radiata* trees grown on a range of soil types. Forest Ecology & Management 135:63-71.

Moore, J.R., B. Gardiner, D. Sellier. 2018. Tree mechanics and wind loading. Pages79-106 in A. Geitmann & J. Gril, editors, **Plant Biomechanics: From Structure to Function at Multiple Scales**. Springer, Cham, Switzerland. Pp.441.

Moulia, B., R. Bastien, H. Chauvet-Thiry, N. Leblance-Fournier. 2019. Posture control in land plants: Growth, position sensing, proprioception, balance, and elasticity. Journal of Experimental Botany 79(14):3467-3494.

Nicoll, B.C. & D. Ray. 1996. Adaptive growth of tree root systems in response to wind action and site conditions. Tree Physiology 16:891-898.

Nicoll, B.C., B.A. Gardiner, B. Rayner, & A.J. Peace. 2006. Anchorage of coniferous trees in relation to species, soil type, and rooting depth. Canadian Journal of Forest Research 36:1871-1883.

Nicoll, B.C., T. Connolly, & B.A. Gardiner. 2019. Changes in spruce growth and biomass allocation following thinning and guying treatments. Forests 10:253-266.

Niez, B., J. Diouha, B. Moulia, E. Badel. 2019. Water-stressed or not, the mechanical acclimation is a priority requirement for trees. Trees: Structure and Function 33:279-291.

Niklas, K.J. 2007. Maximum plant height and the biophysical factors that limit it. Tree Physiology 27:433-440.

Niklas, K.J. & H-C. Spatz. 2012. **Plant Physics**. University of Chicago Press, Chicago, IL. Pp.426.

Ozden, S., R. Ennos. 2018. The mechanics and morphology of branch and coppice stems in three temperate tree species. Trees: Structure and Function 32:933-949.

Paz, H., F. Vega-Ramos, F. Arreola-Villa. 2018. Understanding hurricane resistance nd resilience in tropical dry forest trees: A functional traits approach. Forest Ecology & Management 426:115-122.

Peltola, H., S. Kellomaki, A. Hassinen, M. Granander. 2000. Mechanical stability of Scots pine, Norway spruce and birch: An analysis of tree-pulling experiments in Finland. Forest Ecology and Management 135:143-153.

Peltola, H.M. 2006. Mechanical stability of trees under static loads. American Journal of Botany 93(10):1501-1511.

Peterson, C.J., G.H.P.dM. Ribeiro, R. Negron-Juarez, D.M. Marra, J.Q. Chambers, N. Higuchi, A. Lima, & J.B. Cannon. 2019. Critical wind speeds suggest wind could be an important disturbance agent in Amazonian forests. Forestry 92:444-459.

Rodriguez, M., E. de Langre, B. Moulia. 2008. A scaling law for the effects of architecture and allometry on tree vibration modes suggests a biological tuning to modal compartmentalization. American Journal of Botany 95(12):1523-1537.

Rudnicki, M., S.J. Mitchell, M.D. Novak. 2004. Wind tunnel measurements of crown streamlining and drag relationships for three conifer species. Canadian Journal of Forest Research 34:666-676

Sagi, P., T. Newson, C. Miller, & S. Mitchell. 2019. Stem and root system response of a Norway spruce tree (*Picea abies*) under static loading. Forestry 92:460-472.

Skatter, S., B. Kucera. 2000. Tree breakage from torsional wind loading due to crown asymmetry. Forest Ecology and Management 135:97-103.

Stubbs, C.J., D.D. Cook, K.J. Niklas. 2019. A general review of the biomechanics of root anchorage. Journal of Experimental Botany 70(14):3439-3451.

Telewski, F.W. & J.R. Moore. 2016. Trait selection to improve wind-firmness in trees. CAB Reviews 11(050):1-10.

Thibaut, B. 2019. Three-dimensional printing, muscles, and skeleton: Mechanical functions of living wood. Journal of Experimental Botany 70(14):3453-3466.

Urata, T., M. Shibuya, A. Koizumi, H. Torita, J.Y. Cha. 2012. Both stem and crown mass affect tree resistance to uprooting. Journal of Forest Research 17:65-71.

ver Planck, N.R. & D.W. MacFarlane. 2019. Branch mass allocation increases wind throw risk for *Fagus grandifolia*. Forestry 92:490-499.

Virot, E., A. Ponomarenko, E. Dehandschoewercker, D. Quere, C. Clanet. 2016. Critical wind speed at which trees break. Physical Review E 93:023001

Vollsinger, S., S.J. Mitchell, K.E. Byrne, M.D. Novak, M. Rudnicki. 2005. Wind tunnel measurements of crown streamlining and drag relationships for several hardwood species. Canadian Journal of Forest Research 35:1238-1249.

Watson, A. 2000. Wind-induced forces in the near-surface lateral roots of radiata pine. Forest Ecology and Management 135:133-142.

Wu, T., P. Zhang, L. Zhang, G.G. Wang, M. Yu. 2016. Morphological response of eight *Quercus* species to simulated wind load. PloS ONE 11(9):e0163613.

Wu, Y. & Z. Shao. 2016. Measurement and mechanical analysis of the strains-stresses induced by tree pulling experiments in tree stems. Trees: Structure & Function 30:675-684.

Citation:

Coder, Kim D. 2021. Tree Biomechanics: Basic Understandings Of Structure & Load. University of Georgia, Warnell School of Forestry & Natural Resources Outreach Manual WSFNR21-78A. Pp.50.

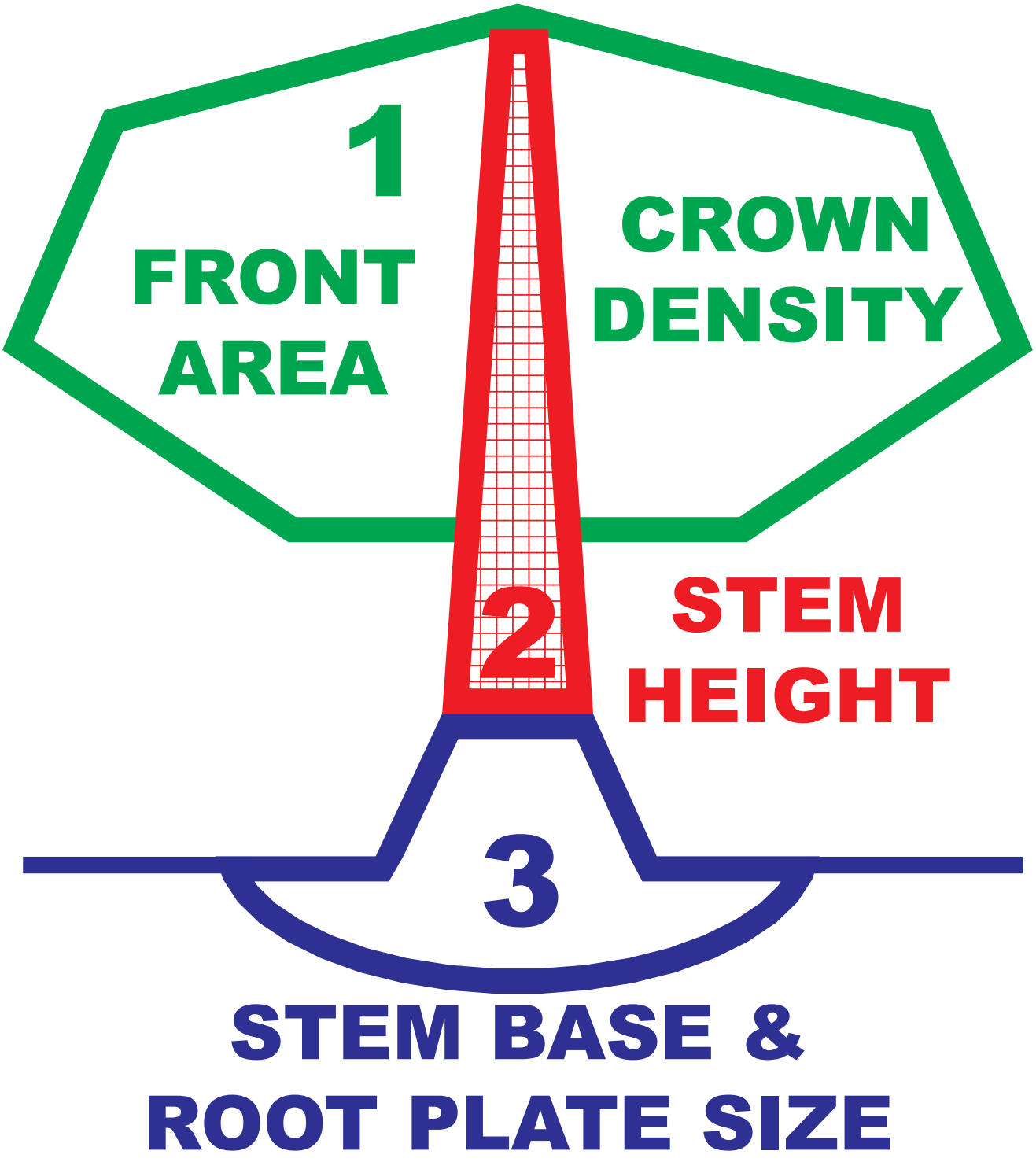

Figure 1: Three primary structural components in trees (sail, height, size) optimized to maintain a tree upright against gravity and wind induced loads.

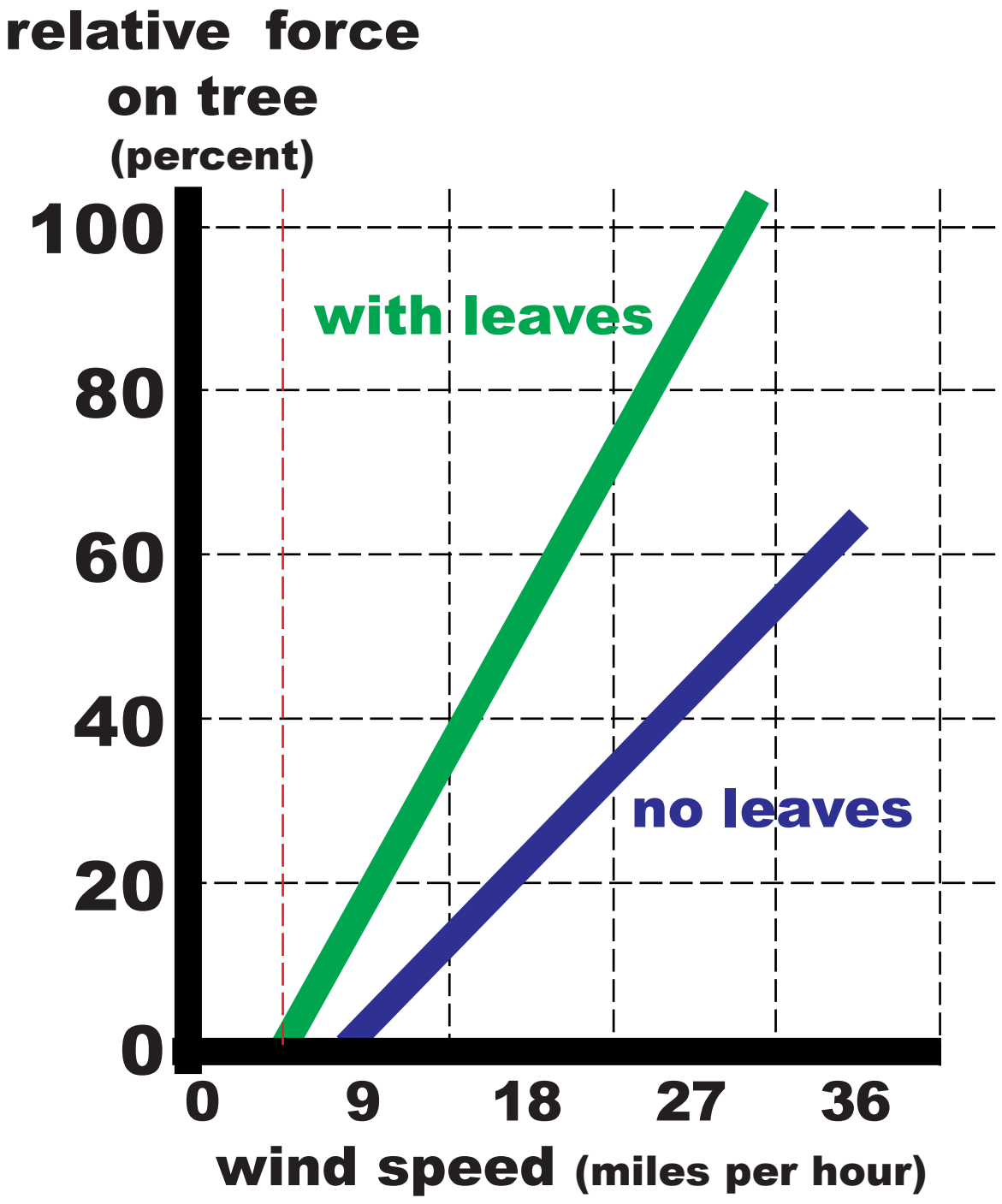

Figure 2: Wind generated force on trees, with and without leaves, as wind speed increases.
(after Angelou et al. 2019)

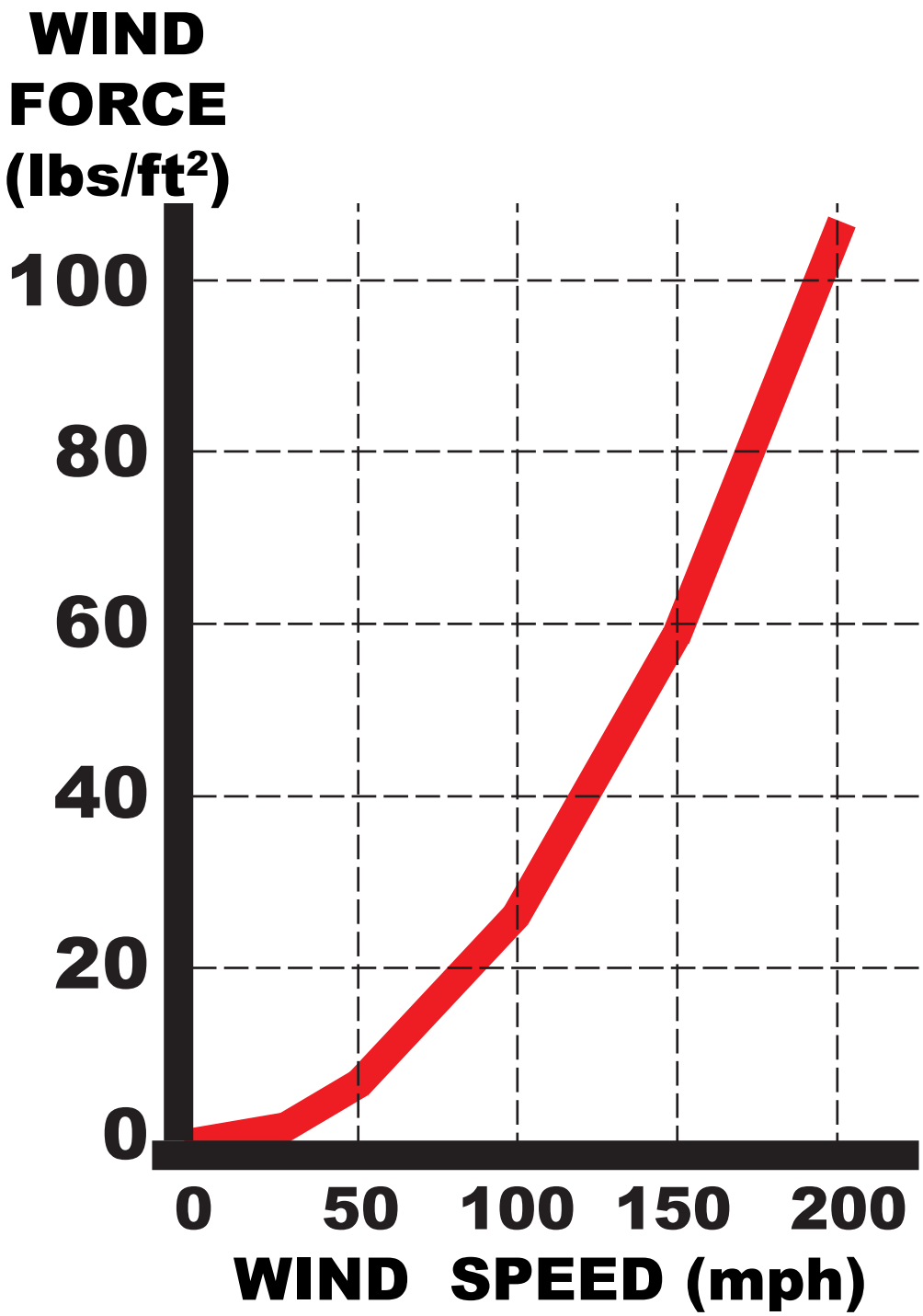

Figure 3: Estmated pressure or force of wind at different wind speeds applied to frontal area of trees. (drag coefficient = 1.0)

wind pressure in pounds per square feet =
(0.013) X (wind speed in miles per hour X (0.45))^2
(Coder 2021d)

wind velocity (mph)	pounds per square feet (lbs/ft²)	wind velocity (mph)	pounds per square feet (lbs/ft²)
5	0.1	80	17
10	0.3	85	19
15	0.6	90	21
20	1.1	95	24
25	1.7	100	26
30	2.4	110	32
35	3.2	120	38
40	4.2	130	45
45	5.3	140	52
50	6.6	150	59
55	8.0	175	81
60	9.5	200	105
65	11	225	133
70	13	250	165
75	15	275	199

wind pressure in pounds per square foot = (0.013) X (wind speed in mph X (0.45))²
(drag coefficient = 1.0)

Figure 4: Estimated wind pressures in pounds per square feet (lbs/ft²) on tree frontal area calculated under standard conditions for various wind velocities in miles per hour (mph). (Coder 2021d)

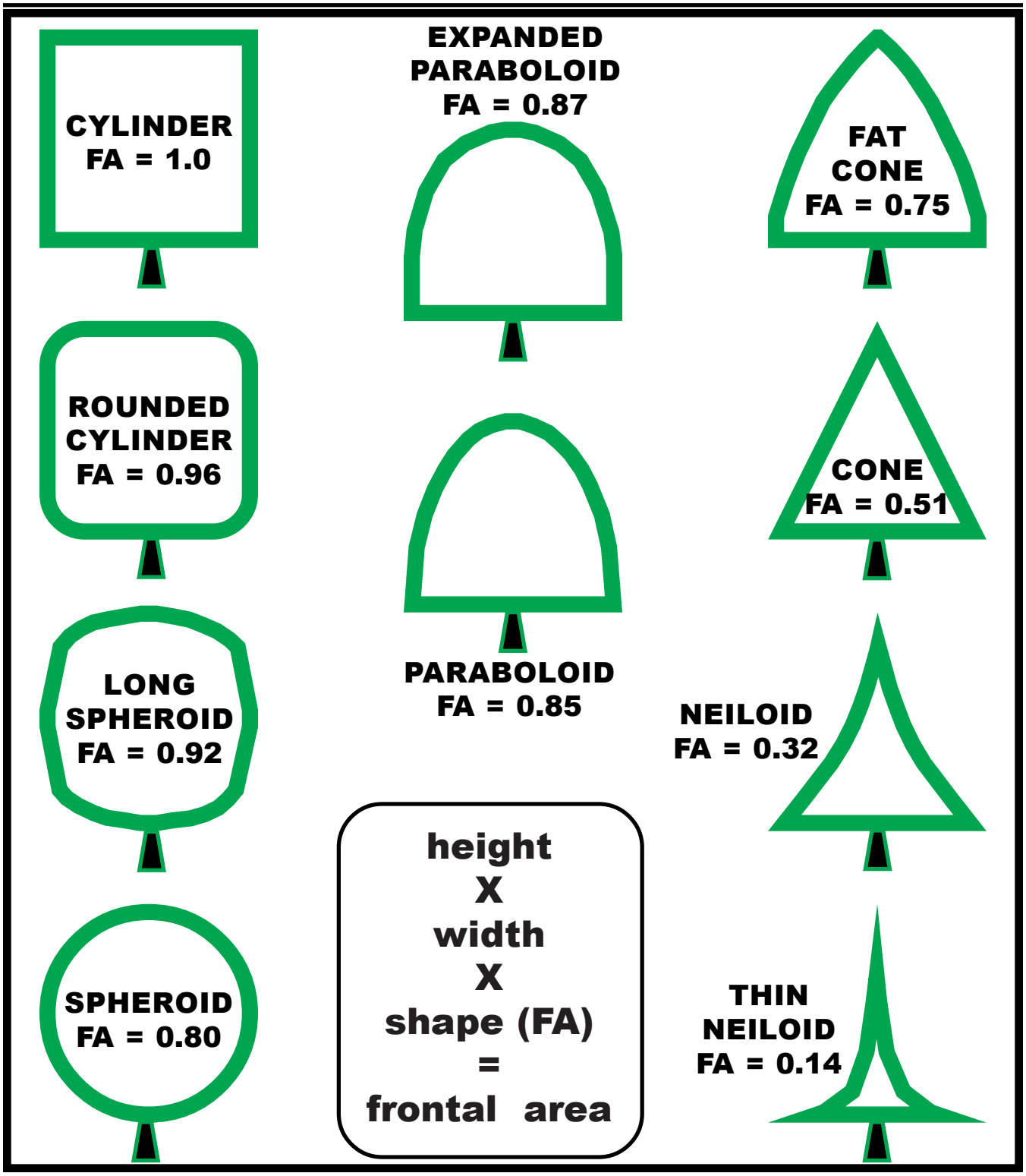

Figure 5: Primary geometric tree crown shapes with relative frontal areas (FA) given under no wind load.

Downwind streamlining and reconfiguration will change frontal area and its shape. All crown shapes have a circular cross-section.

index value	wind speed (mph)	wind pressure (lbs/ft^2)	tree crown reconfiguration descriptor	tree crown reconfiguration value (%)
C0	0	0	gravity impacts only	0 %
CI	10	0.3	petiole & blade deforming, & twig swaying	5 %
CII	19	1.0	leaves rolled back & large peripheral twigs sway	10 %
CIII	28	2.0	twigs pulled back & peripheral branches sway	25 %
CIV	37	3.6	branches pulled back & stem swaying	45 %
CV	46	5.6	twig breakage, stem pushed / held downwind	70 %
CVI	55_{mph}	$8.0_{lbs/ft^2}$	twig & branch breakage (~ T1 threshold – maximum streamlining))	100 %

Figure 6: Index of Tree Crown Reconfiguration giving index value symbol, wind speed in miles per hour, wind pressure in pounds per square feet, tree crown reconfiguration description, and tree crown reconfiguration percentage. (drag coefficient = 1.0)

Note crown reconfiguration under ice plus wind reaches 100% streamlining at CIII (28mph & $2lbs/ft^2$) (Coder 2021d)

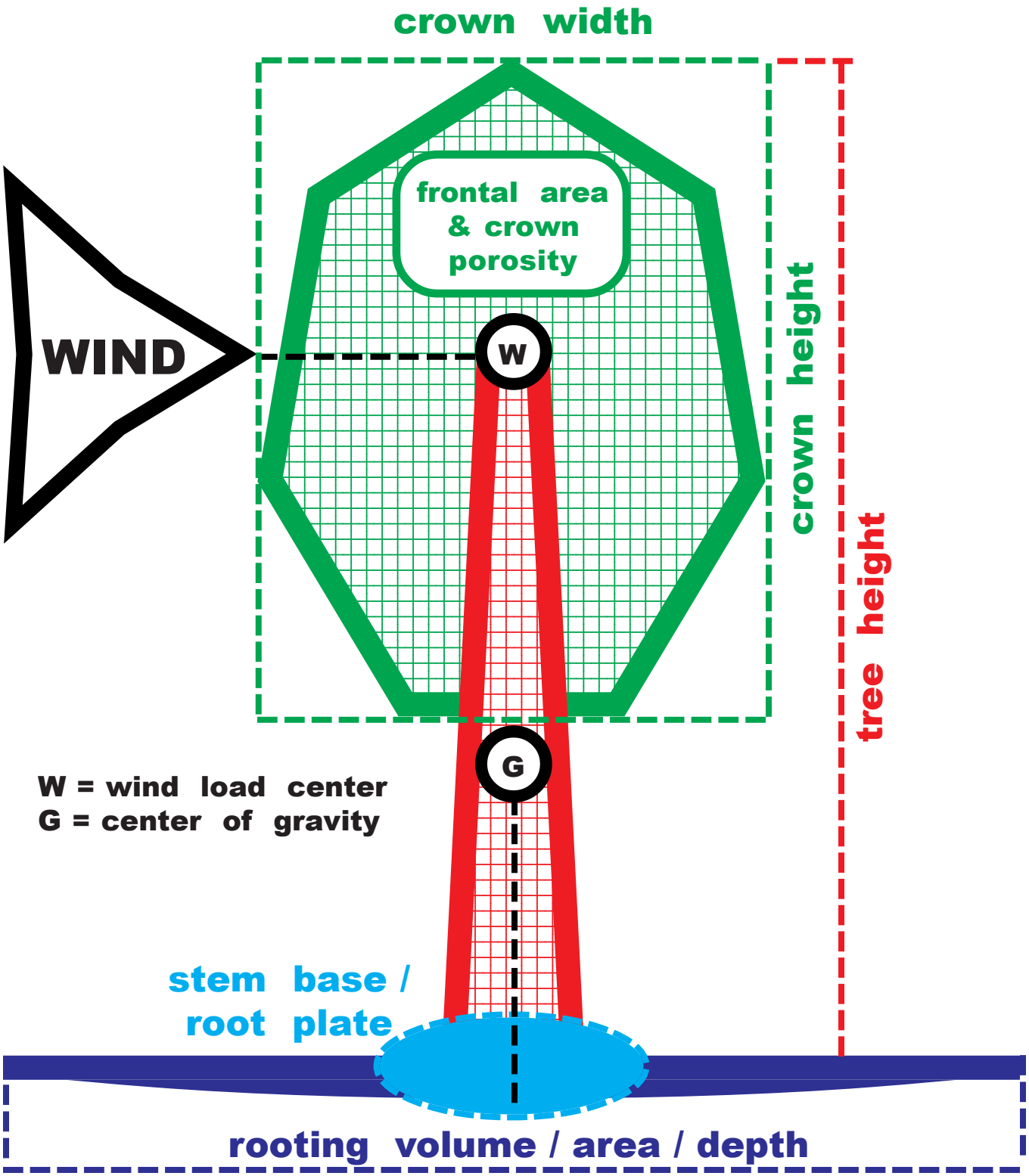

Figure 7: Tree structural model.
(derived from Jelonek et al. 2019)

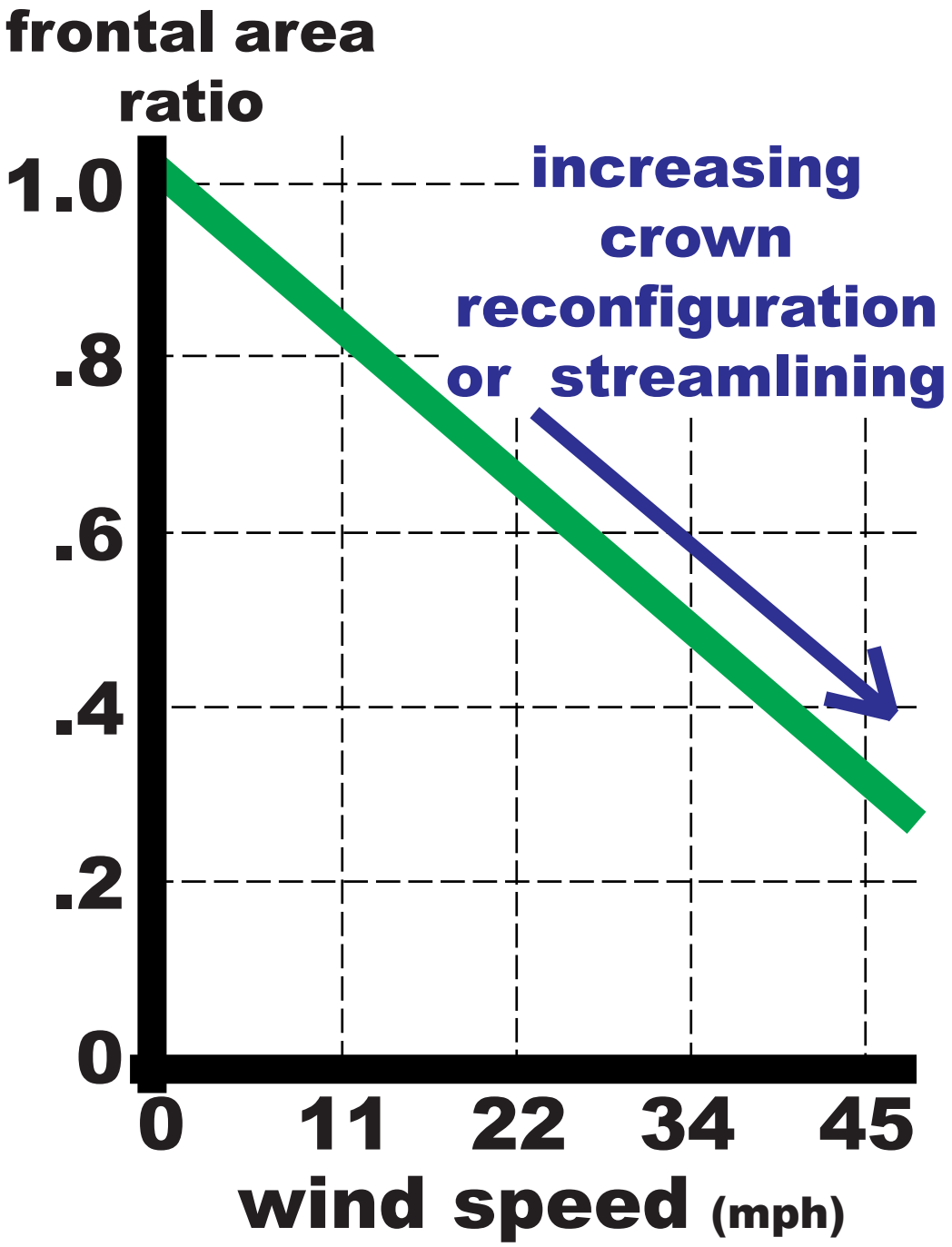

Figure 8: Frontal area ratio (frontal area / still-air frontal area) for unpruned hardwoods versus wind speed.
(after Vollsinger et al. 2005)

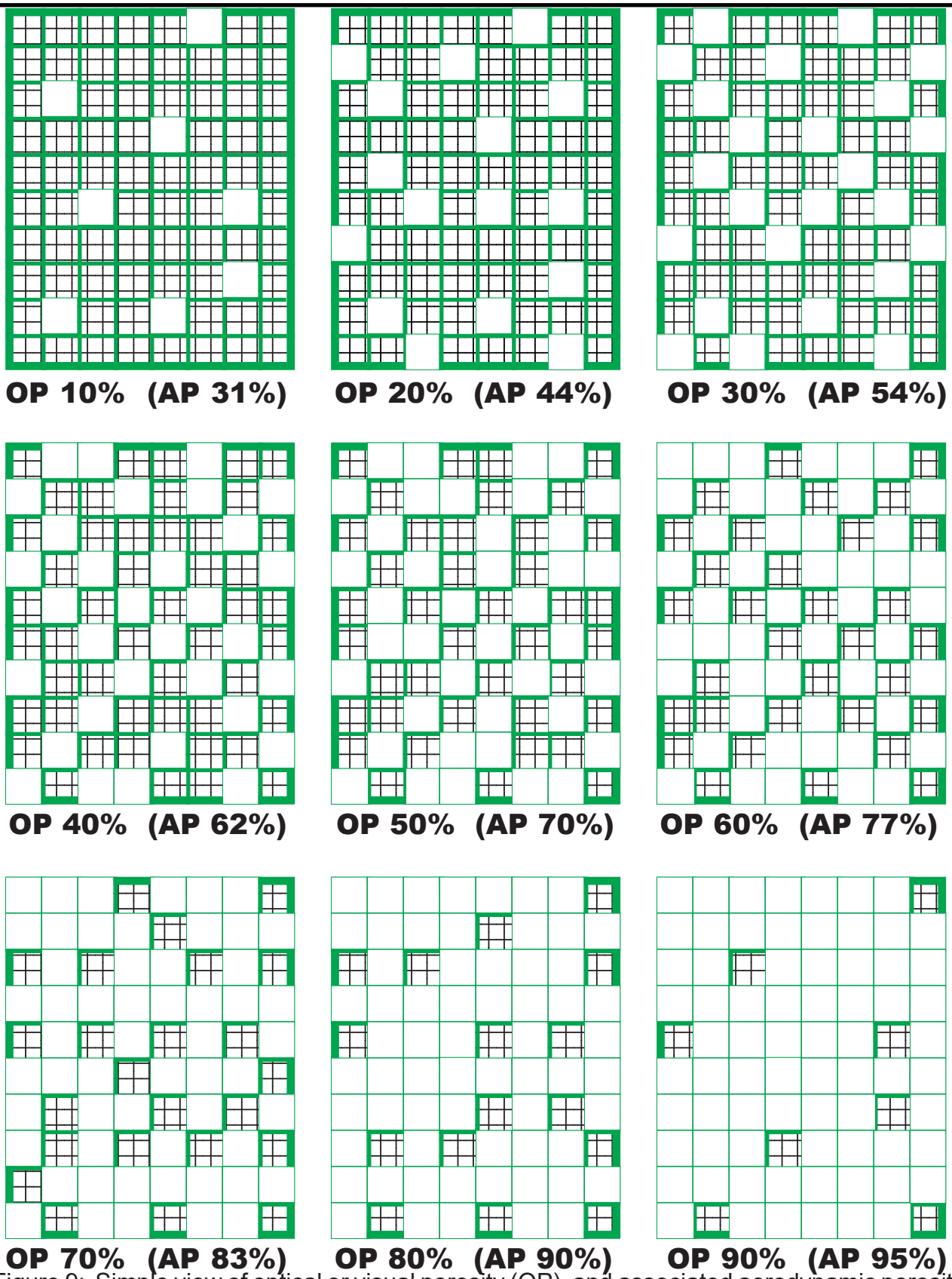

Figure 9: Simple view of optical or visual porosity (OP), and associated aerodynamic porosity (AP), of tree crowns. AP values are average of two formulae -- Gonzales et al. 2018; Manickahan et al. 2018.

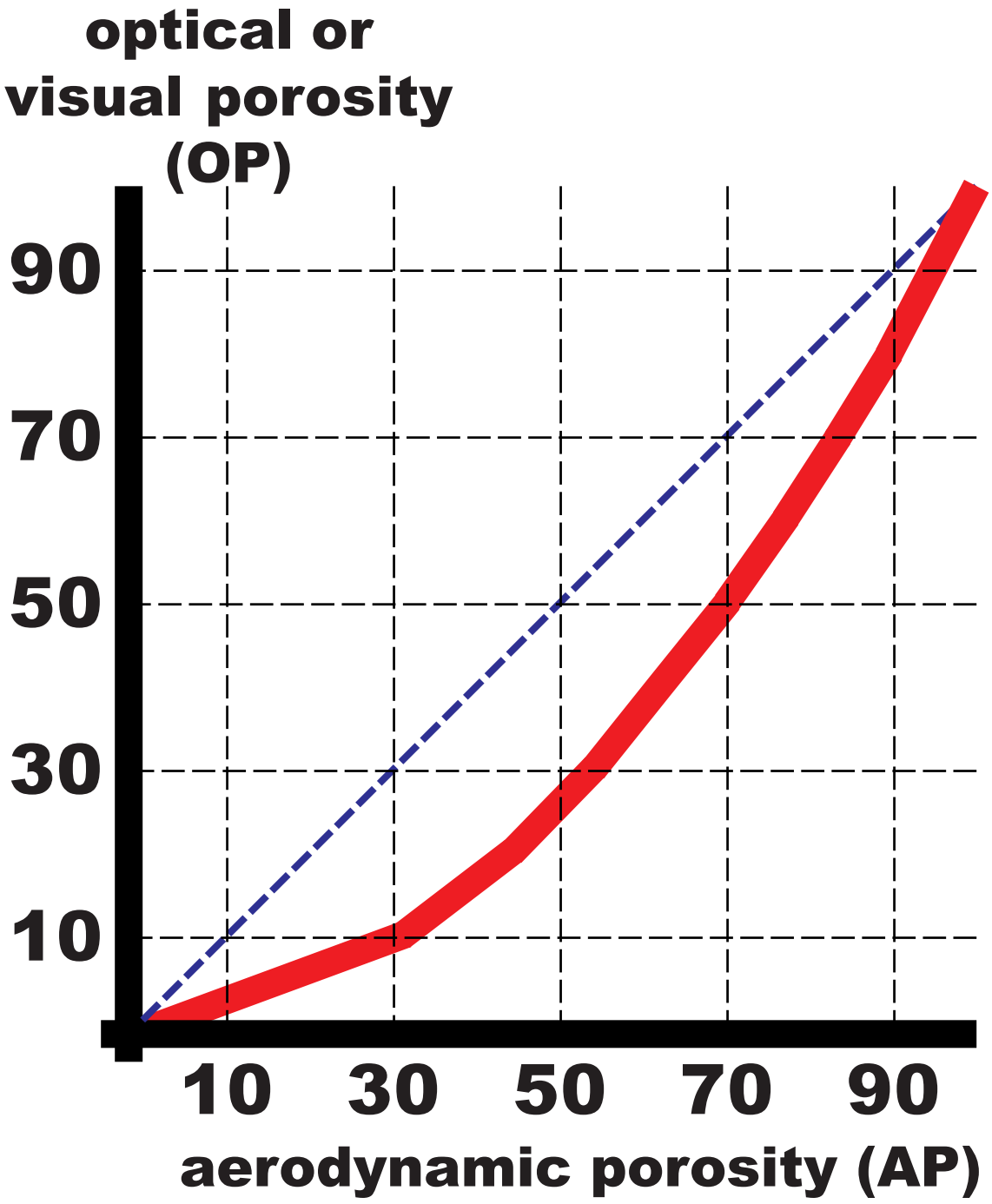

Figure 10: Comparing visual or optical crown porosity (OP) with aerodynamic crown porosity (AP).
Note OP underestimates wind impacts on crowns measured as AP.

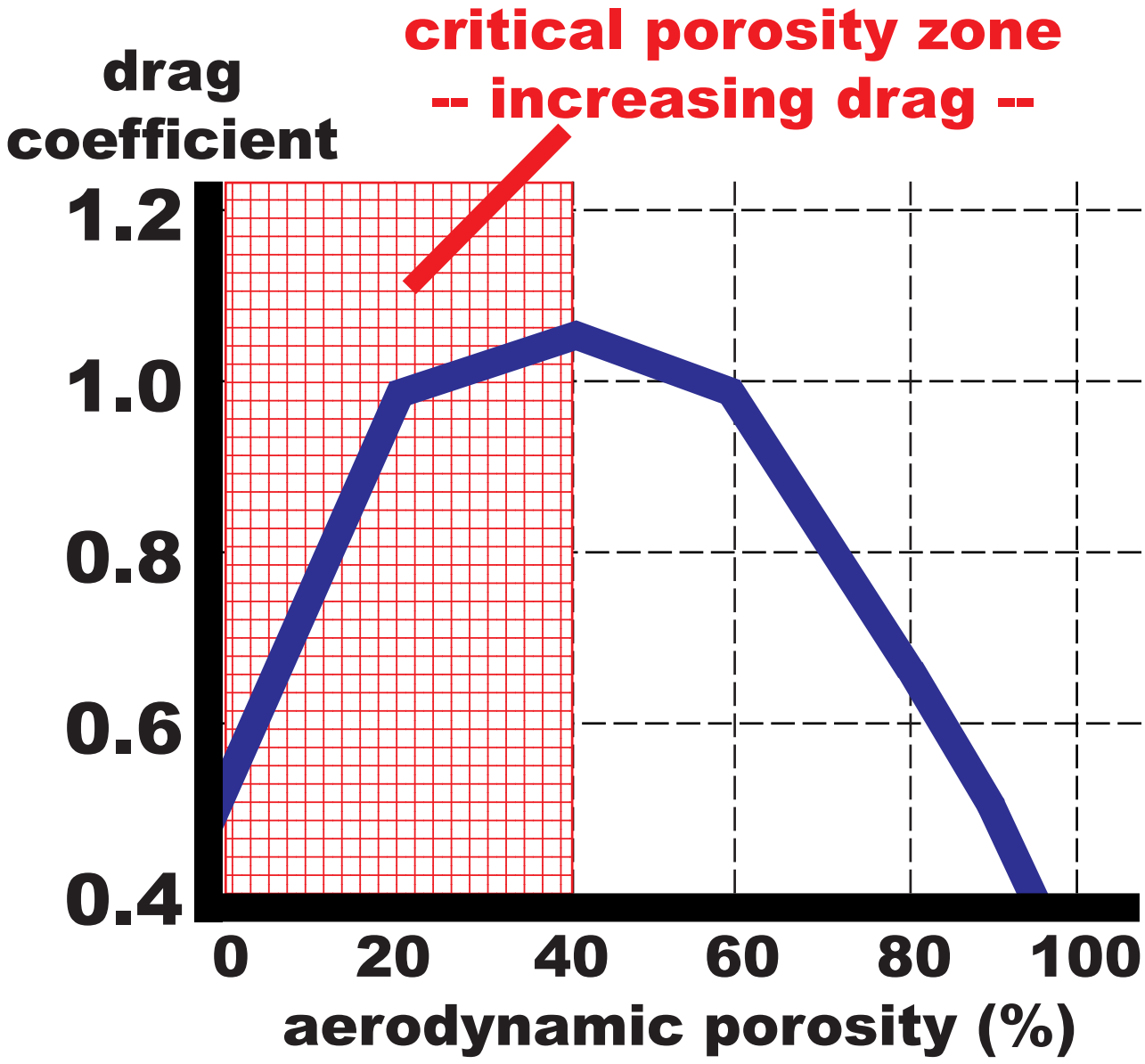

Figure 11: Comparing aerodynamic porosity of tree crowns and tree drag coefficients. (Manickathan et al. 2018)

Drag Coefficients

Gymnosperm -- evergreen

11 mph	0.94	(n=5)
22 mph	0.69	(n=3)
34 mph	0.58	(n=4)
45 mph	0.55	(n=6)
67 mph	0.60	(n=2)

Angiosperm -- deciduous

11 mph	0.60	(n=8)
22 mph	0.49	(n=9)
34 mph	0.42	(n=4)
45 mph	0.38	(n=16)
67 mph	0.20	(n=4)

Angiosperm -- evergreen

11 mph	0.89	(n=1)
22 mph	0.79	(n=1)
34 mph	0.68	(n=1)
45 mph	0.59	(n=1)

Figure 12: Average tree drag coefficients by wind speed (mph).
(n = number of citations)

Vogel Numbers

(theoretical Vogel Exponent = -0.66)

Gymnosperm -- evergreen

-0.31 (n=7)

(range = -0.10 to -0.65)

Angiosperm -- deciduous

-0.40 (n=9)

(range = -0.05 to -1.0)

leaves on = -0.50 (n=3)
leaves off = -0.30 (n=3)

Note, younger trees would have lower (more negative) exponent values due to more effective reconfiguration / streamling than older trees.

Figure 13: Average tree Vogel numbers for use in modifying wind speed exponents, by tree types.

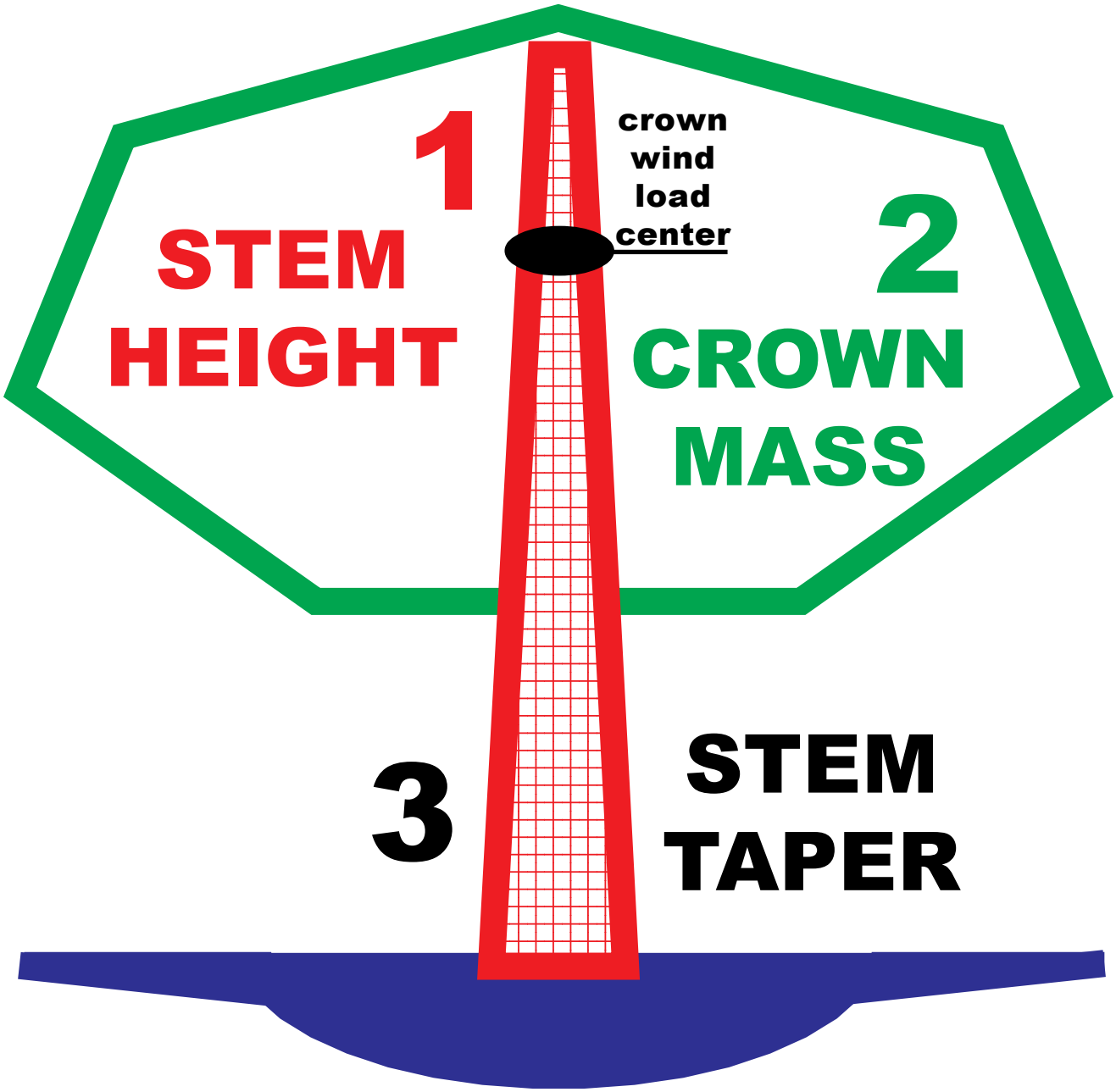

Figure 14: Height related structural components in trees optimized to maintain a tree upright against gravity and wind loads.

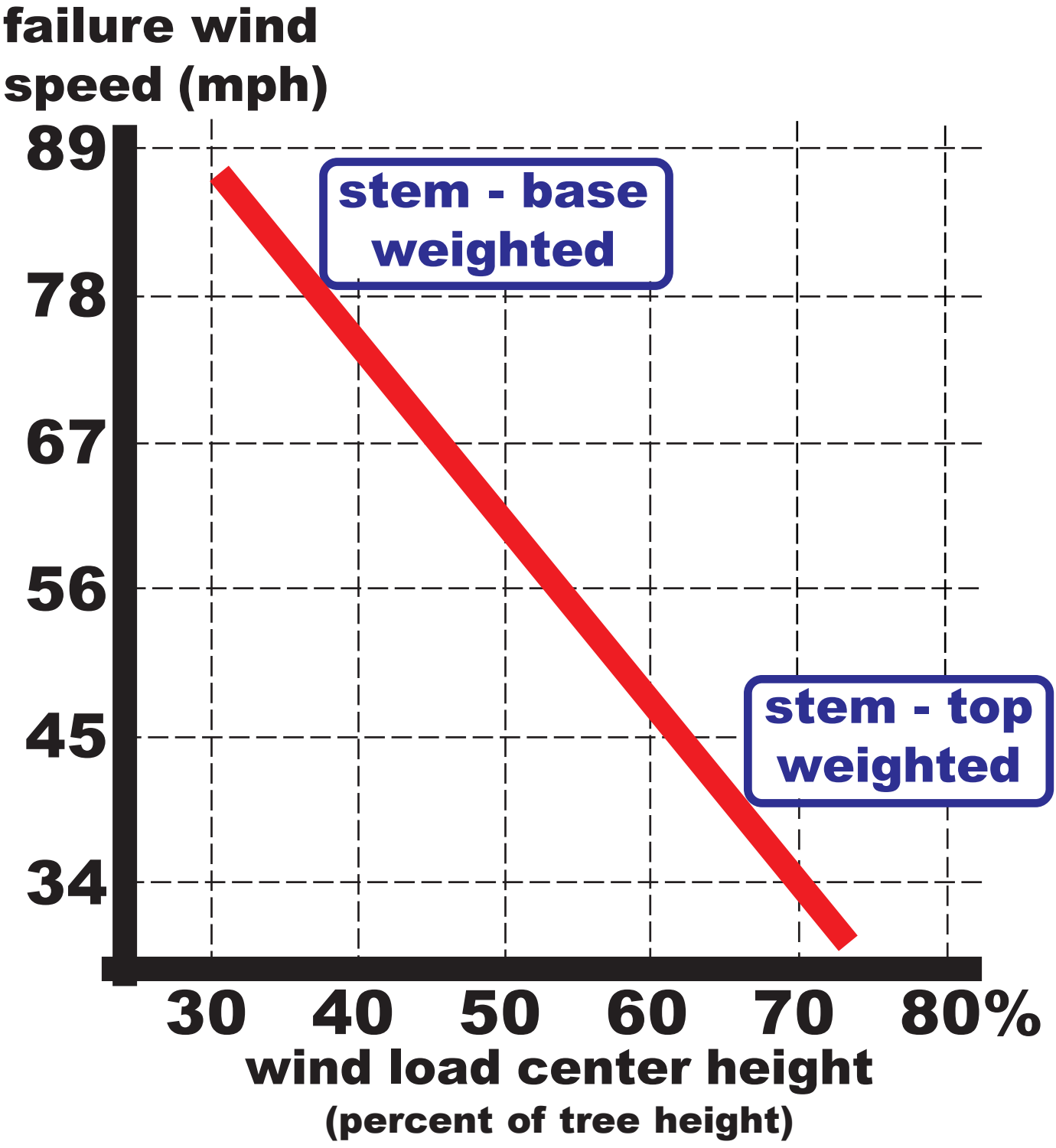

Figure 15: Example tree failure wind speeds versus tree wind load center's height. (after Urata et al. 2012)

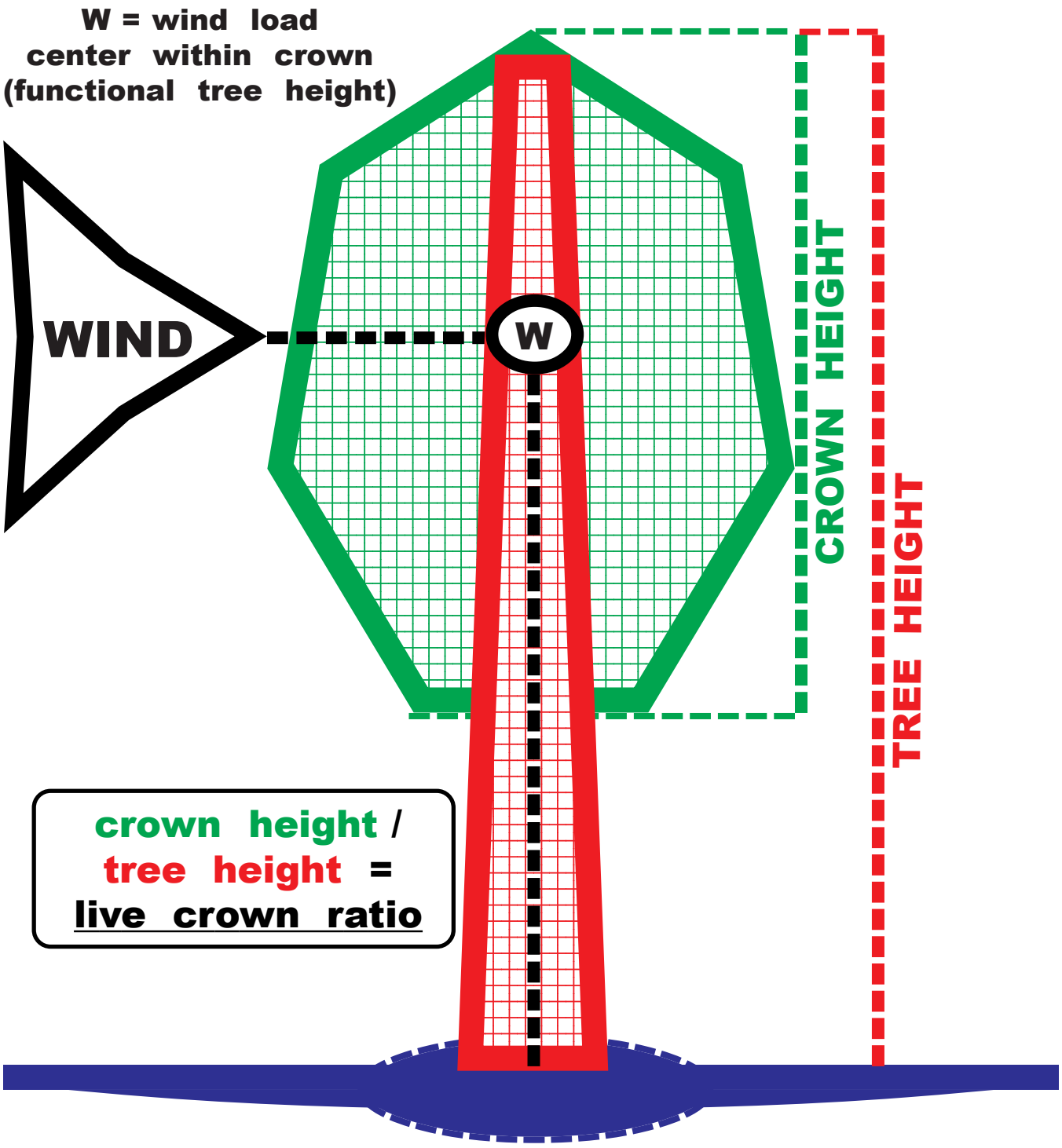

Figure 16: Tree structural model showing total tree height, functional tree height (height of wind load center in crown), and live crown ratio.

(In this image, live crown ratio = 65%)

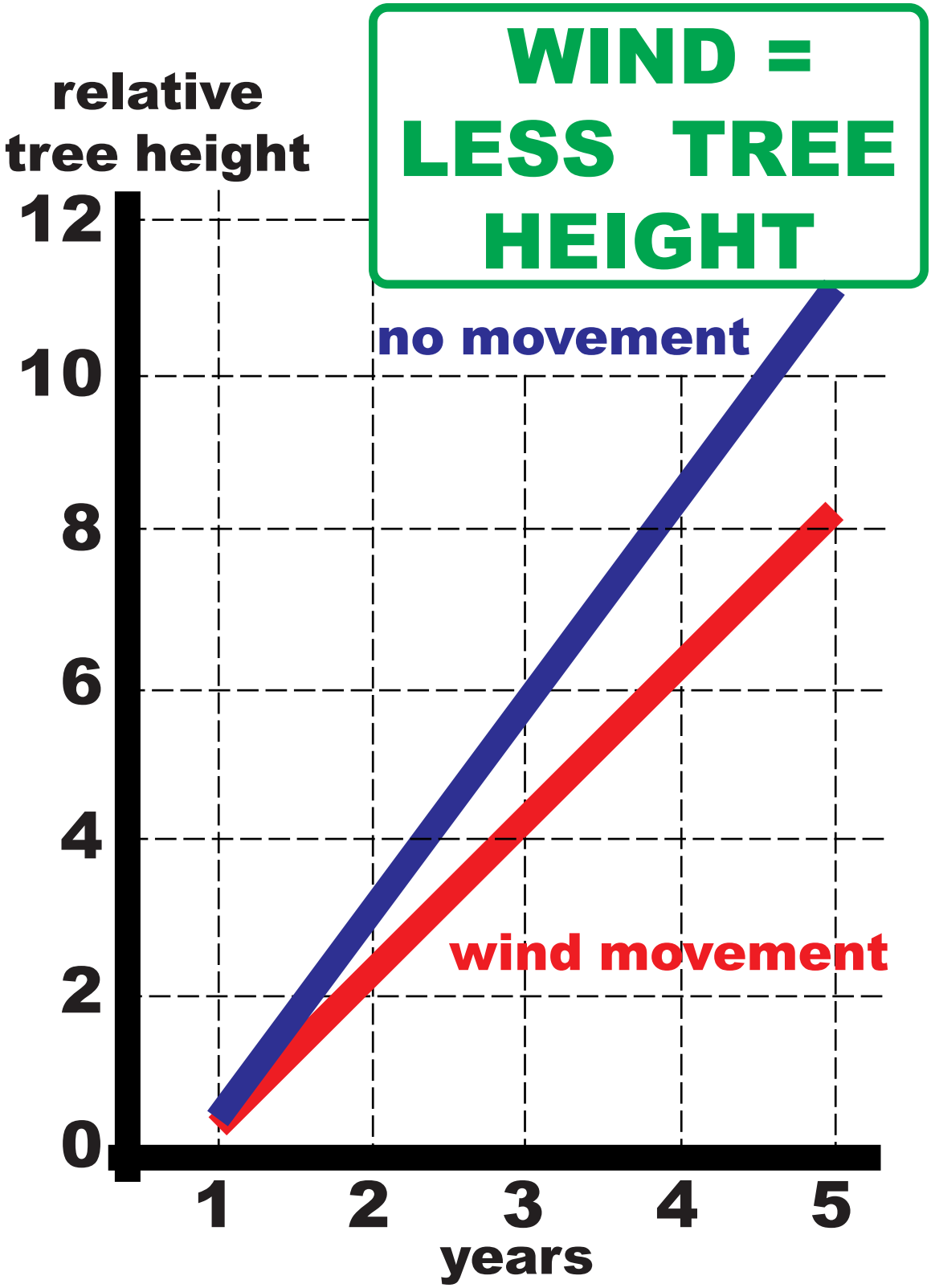

Figure 17: Relative tree height growth when allowed to move in wind compared to a tree constrained from movement. (derived from Nicoll et al. 2019)

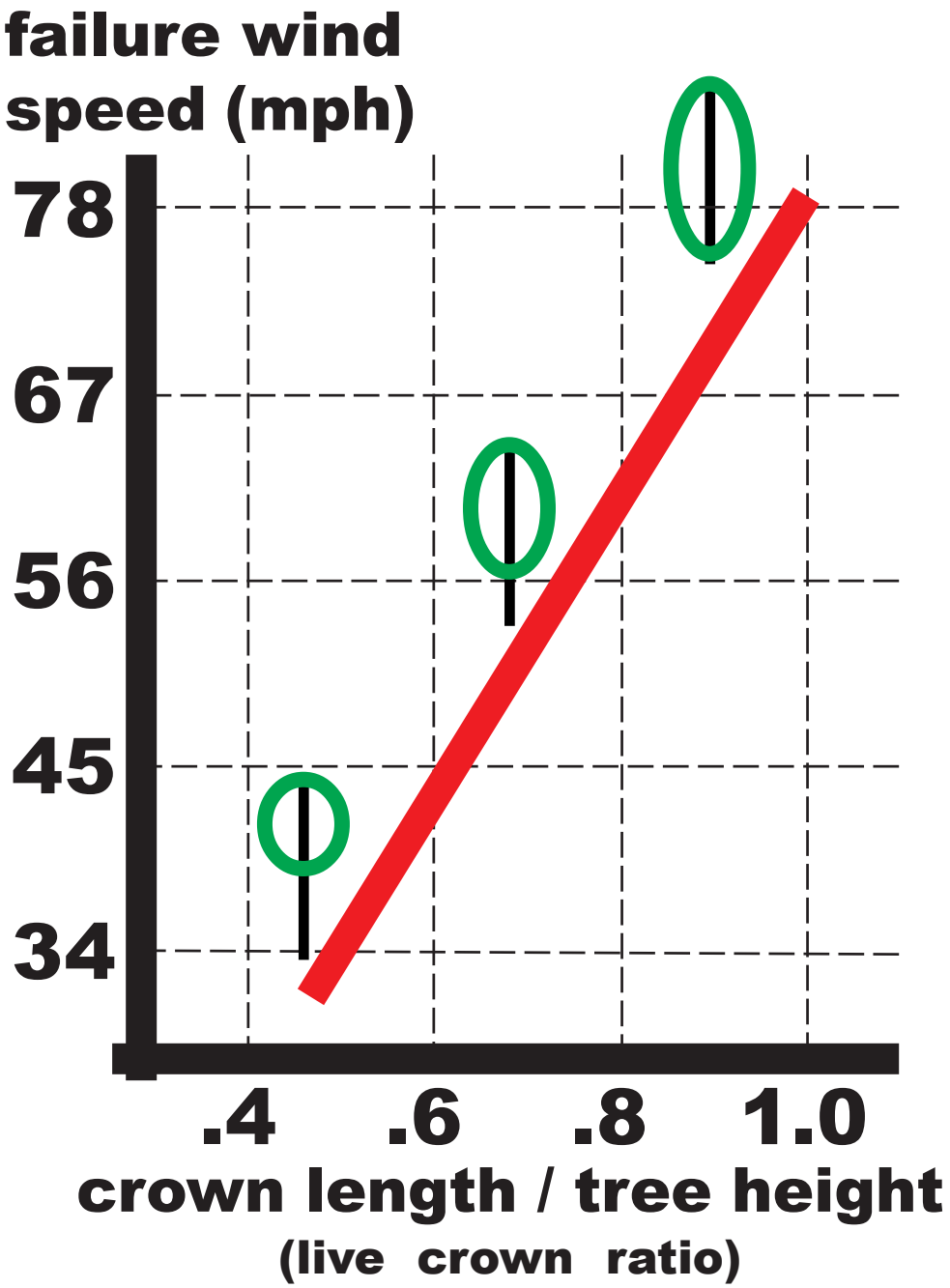

Figure 18: Failure wind speed for a tree versus its crown length / tree height (live crown ratio).
(after Urata et al. 2012)

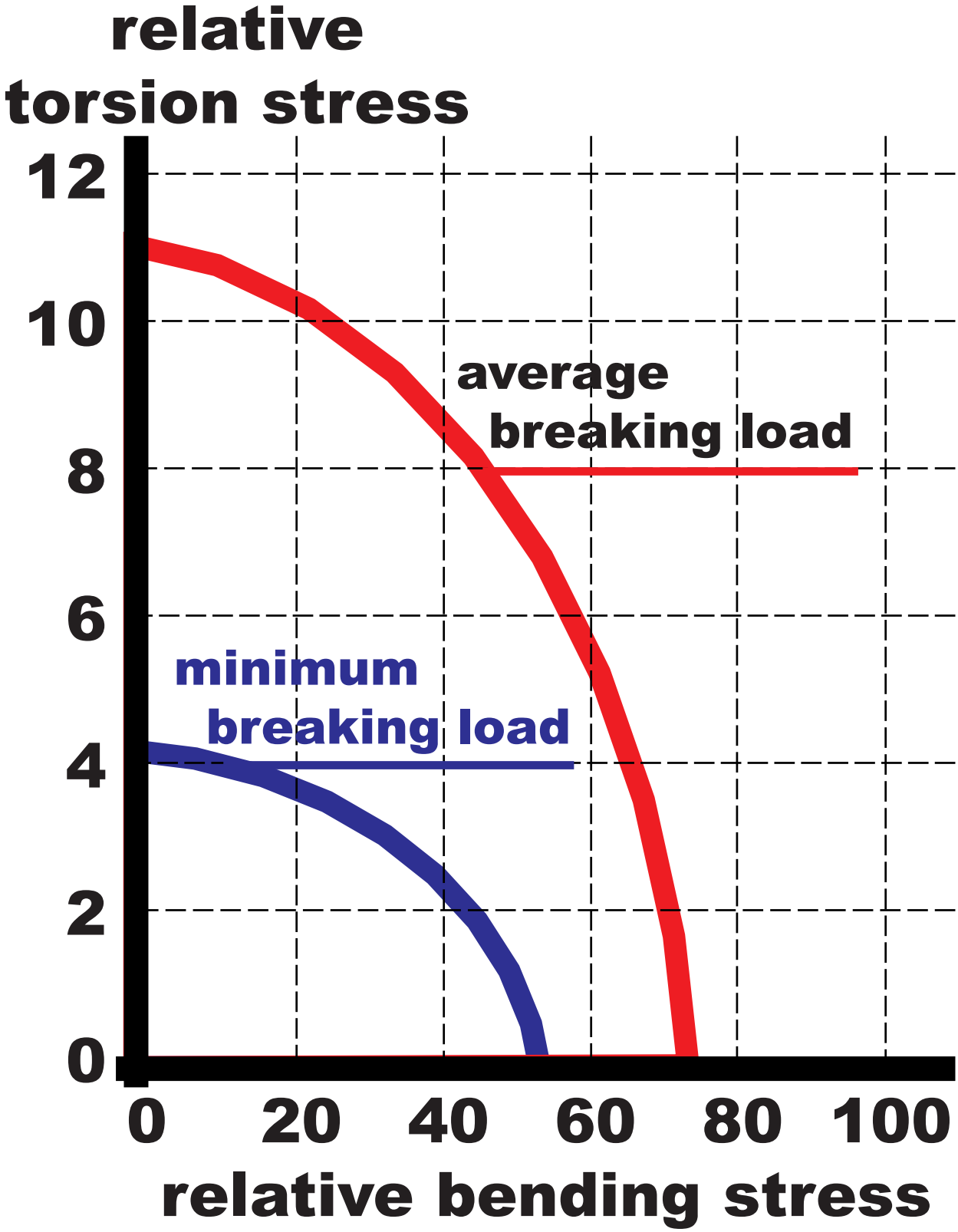

Figure 19: Relationship between relative bending and torsion loads in breaking branches. (Avalos & Sanchez 2014)

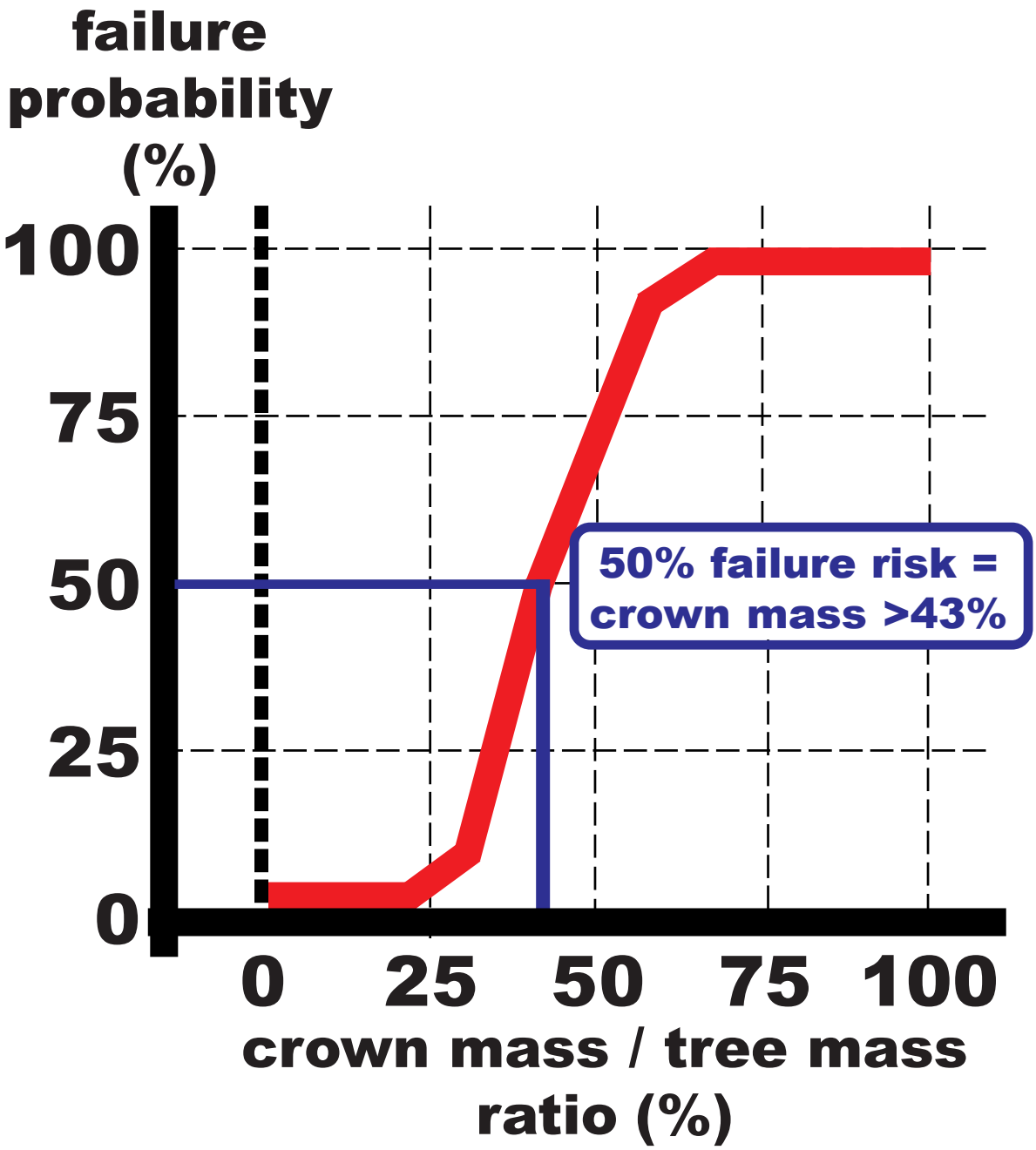

Figure 20: Probability of tree failure based upon crown mass proportion of above-ground tree mass.
(after ver Planck & MacFarlane 2019)

CROWN RAISING

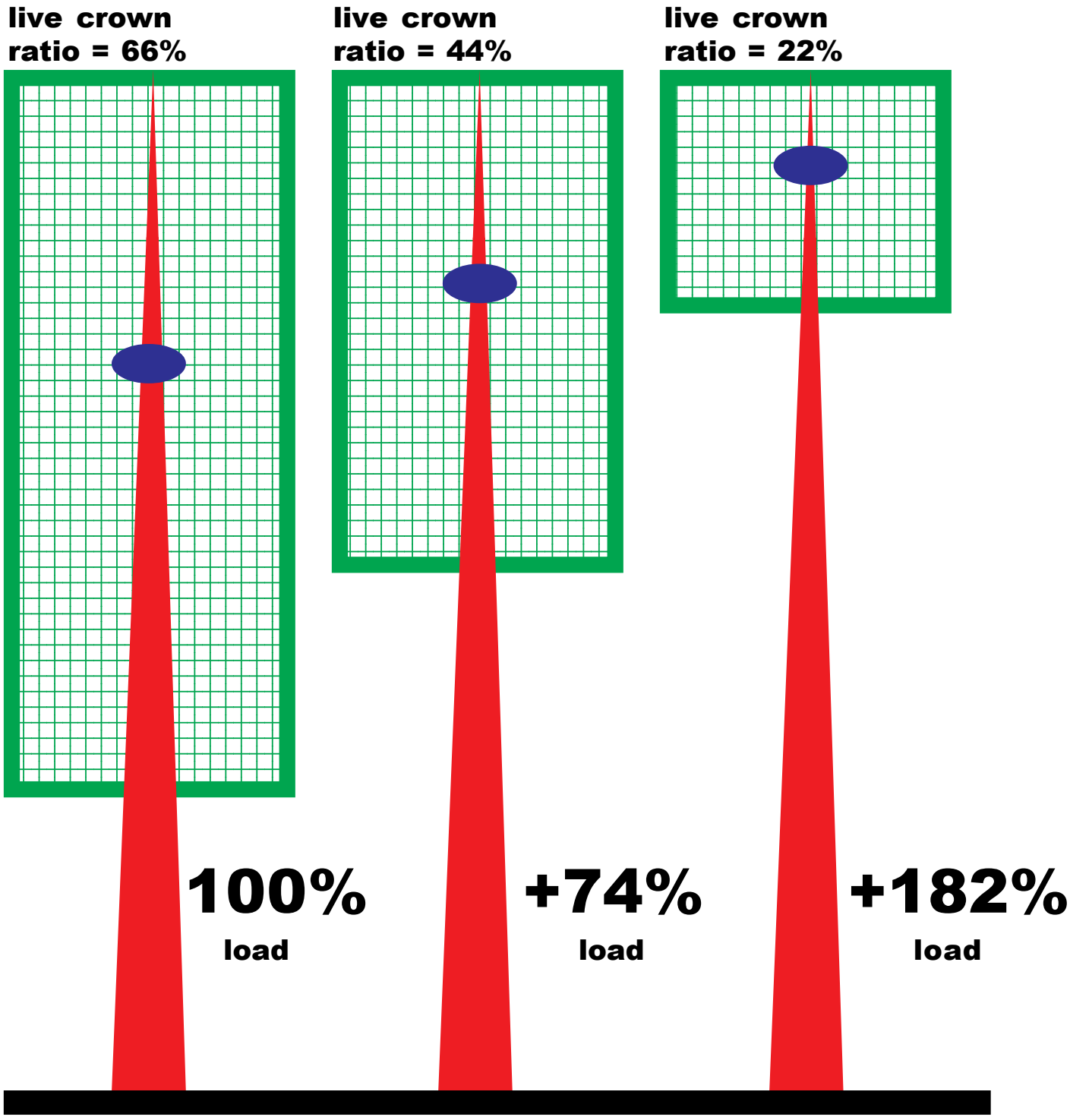

Figure 21: Relative tree wind load increases under two crown raising treatments (1/3 & 2/3). The blue oval is the crown wind load center. (Relative load relationships also apply to large branch treatments.)

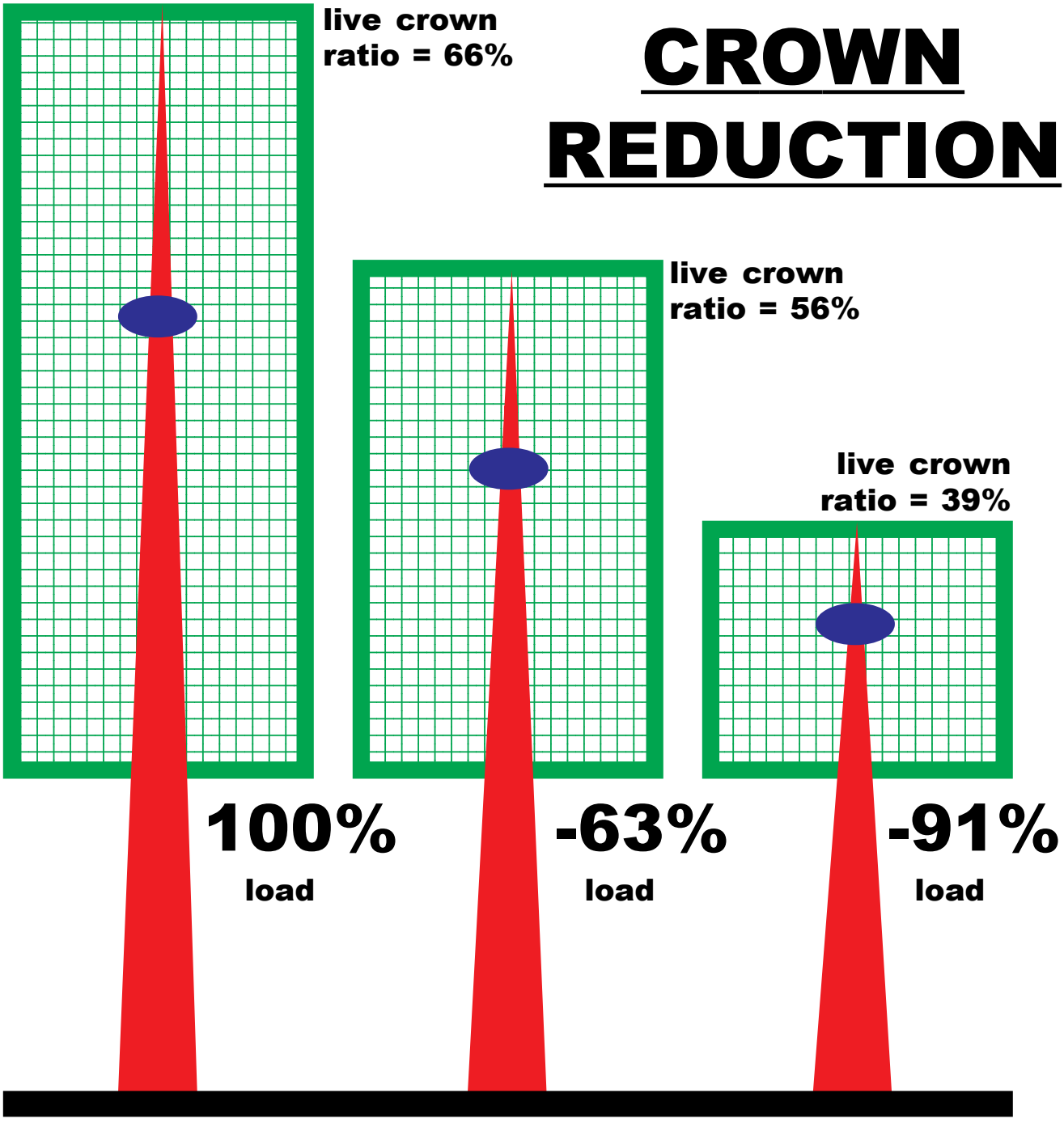

Figure 22: Relative tree wind load decreases under two crown reduction treatments (1/3 & 2/3). The blue oval is the crown wind load center.

(Relative load relationships also apply to large branch treatments.)

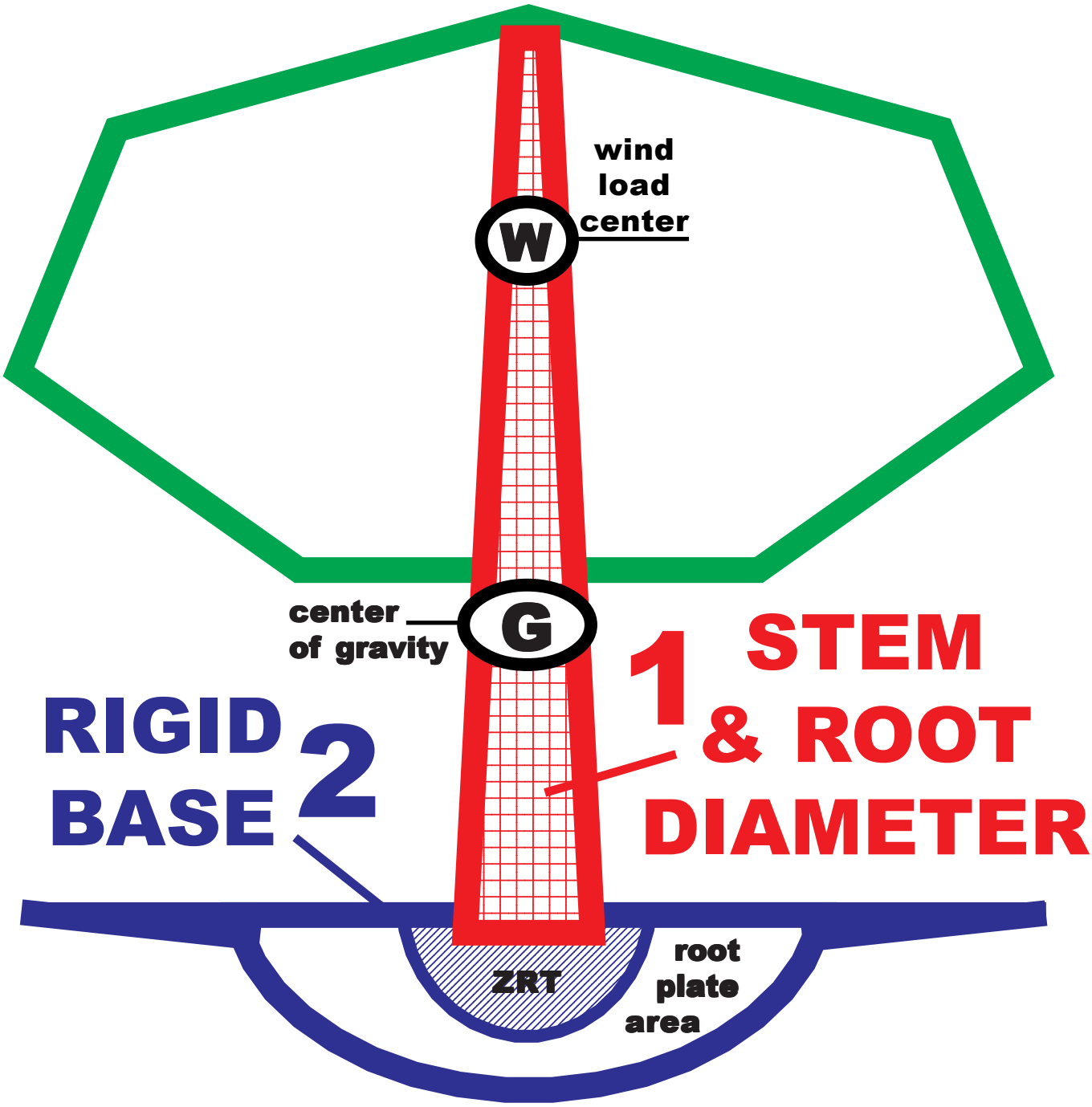

Figure 23: Diameter related structural components optimized to maintain a tree upright against gravity and wind loads.

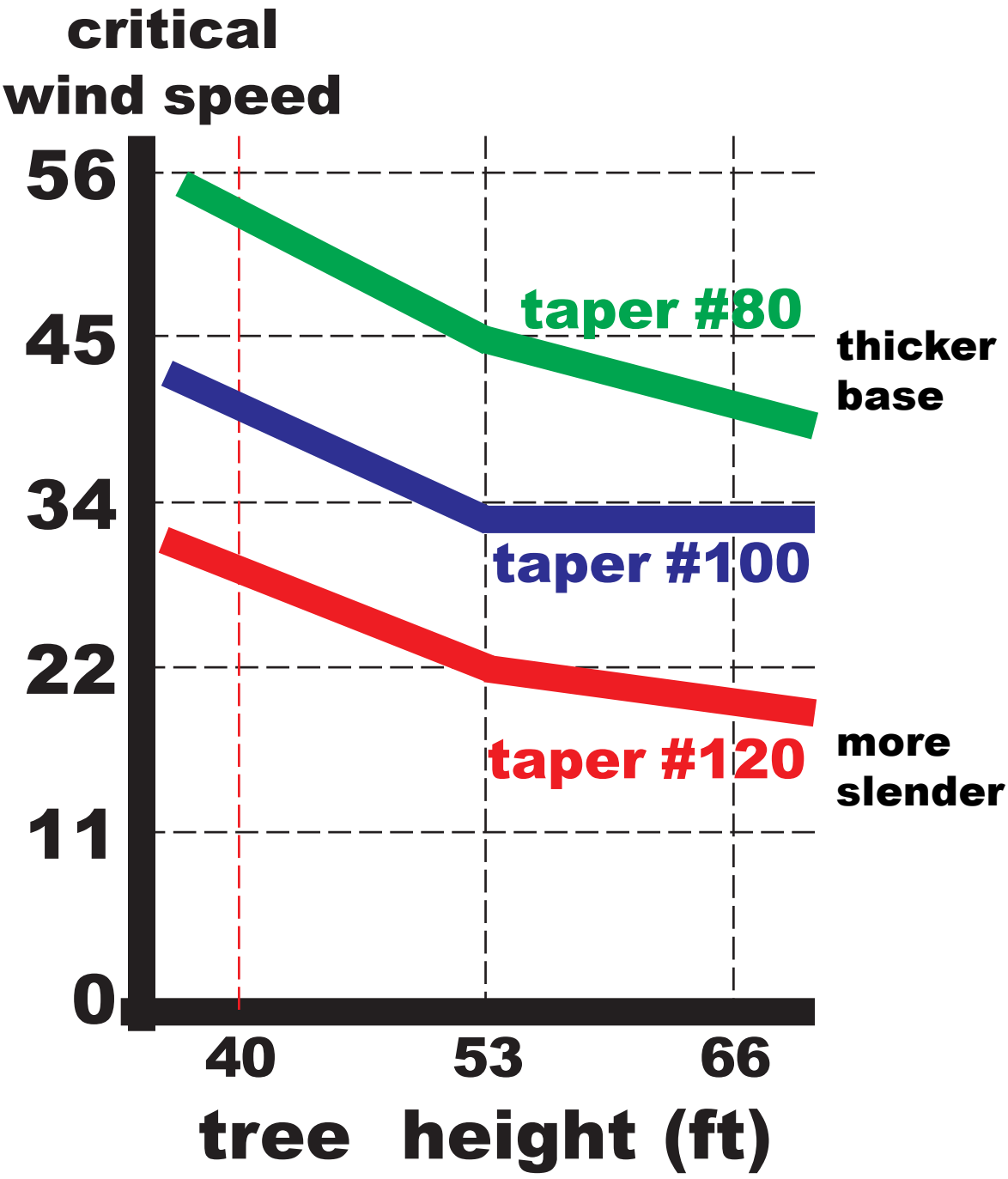

Figure 24: Critical wind speed (mph) measured at 33 feet in height for uprooting trees of different slenderness (height / dbh ratio or taper number).
(after Peltola 2006)

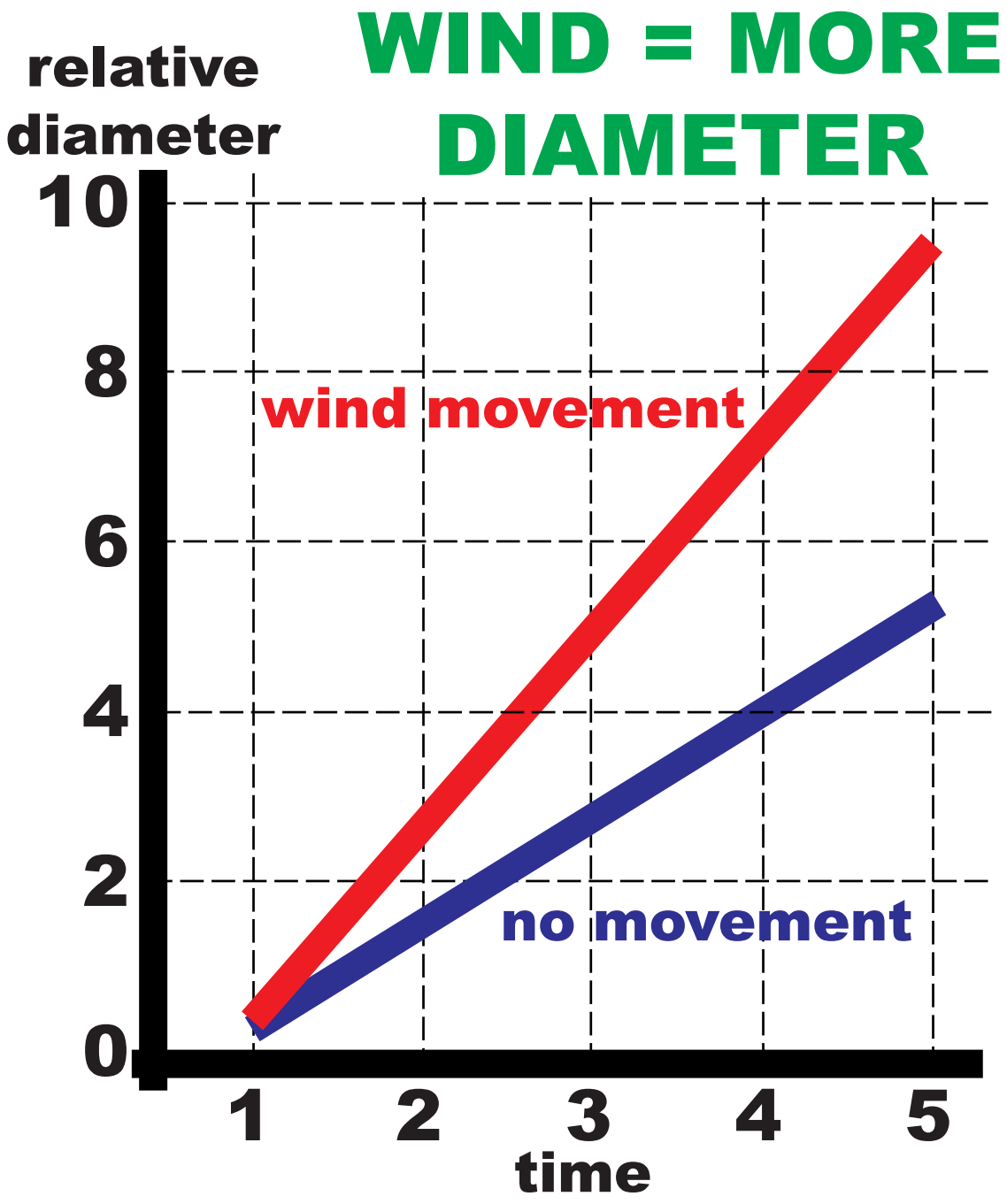

Figure 25: Combined relative stem base diameter growth and basal root diameter growth for trees allowed to move in wind versus trees restrained from movement.
(derived from Nicoll et al. 2019)

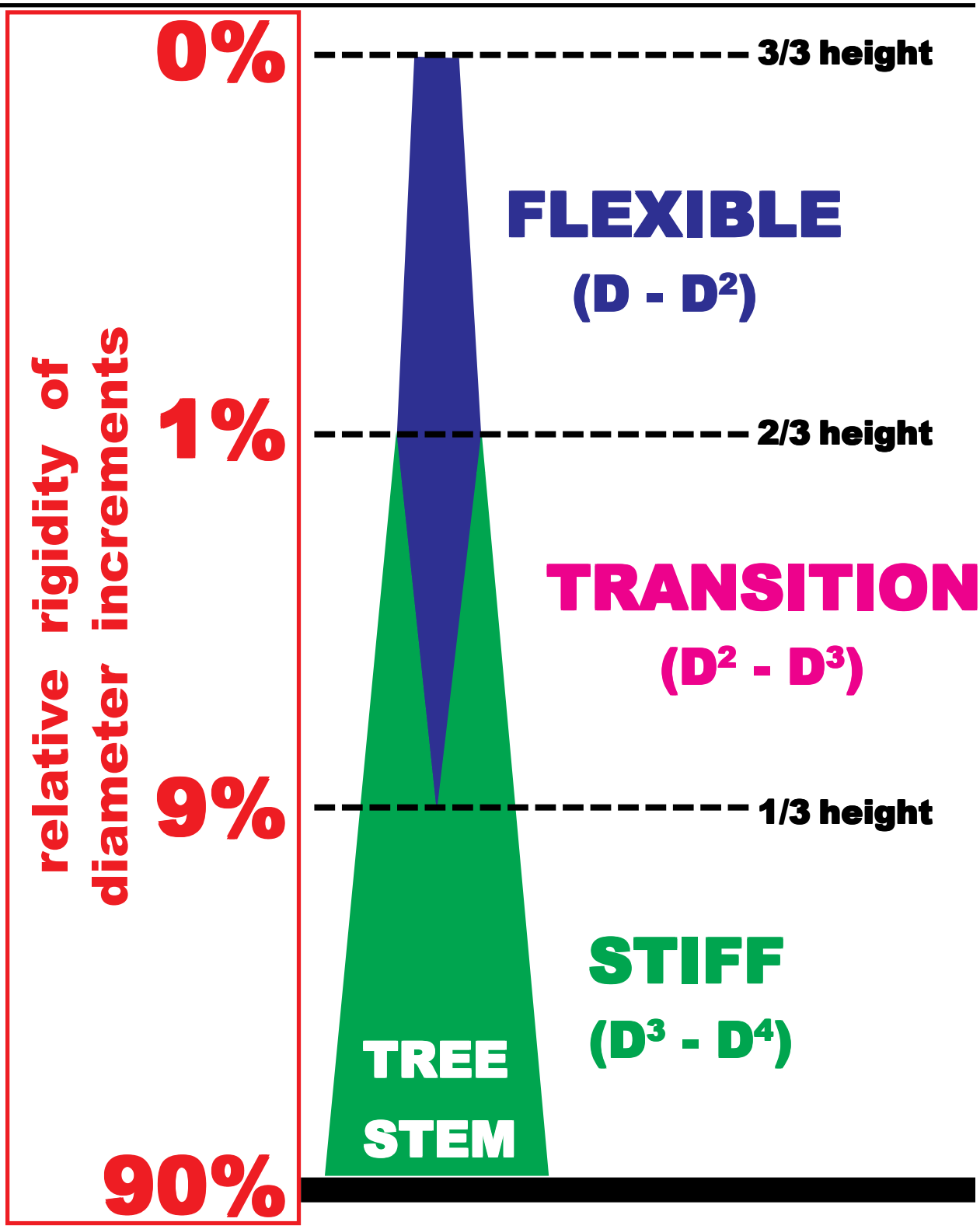

Figure 26: Tree stem stiffness and flexibility zones based upon calculated diameter increment values (D^X) and comparative rigidity of diameter increments at each location.

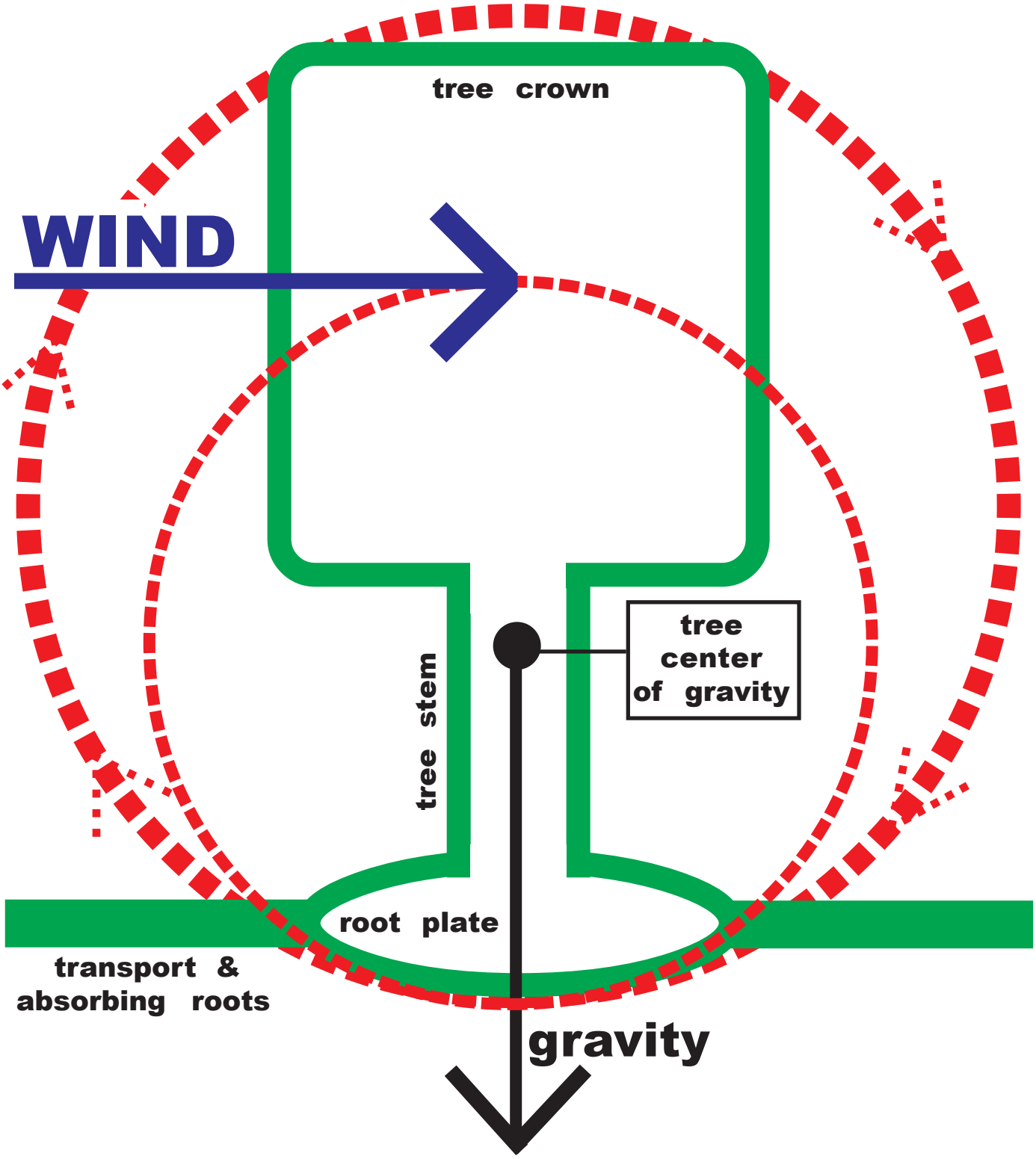

Figure 27: Simplified view of wind and gravity loads acting to rotate a tree out of soil as a combined load wheel.
(Coder 2010; Coder 2018)

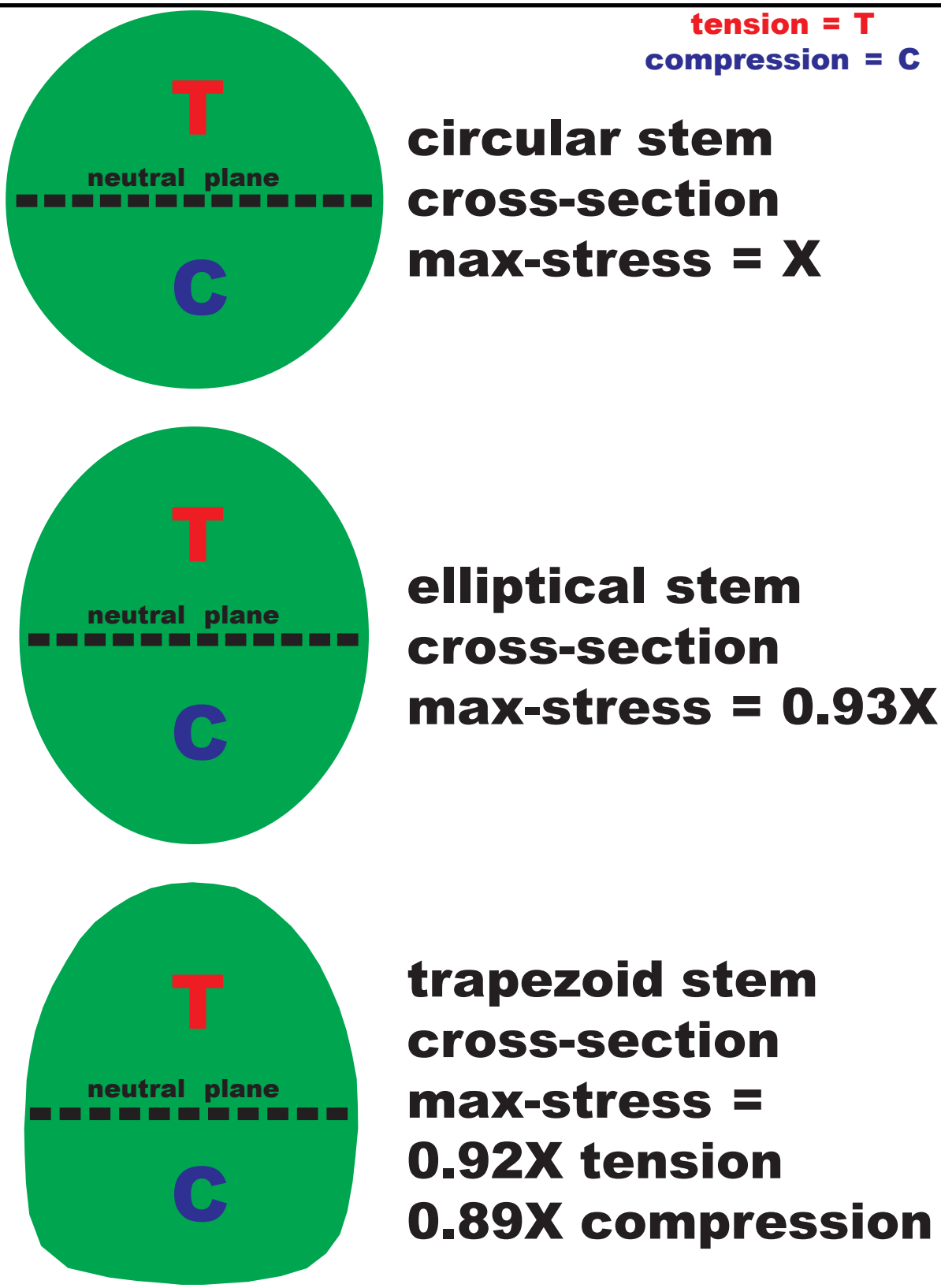

Figure 28: Tree stem cross-sectional shapes impact on maximum stress. (Niez et al. 2019)

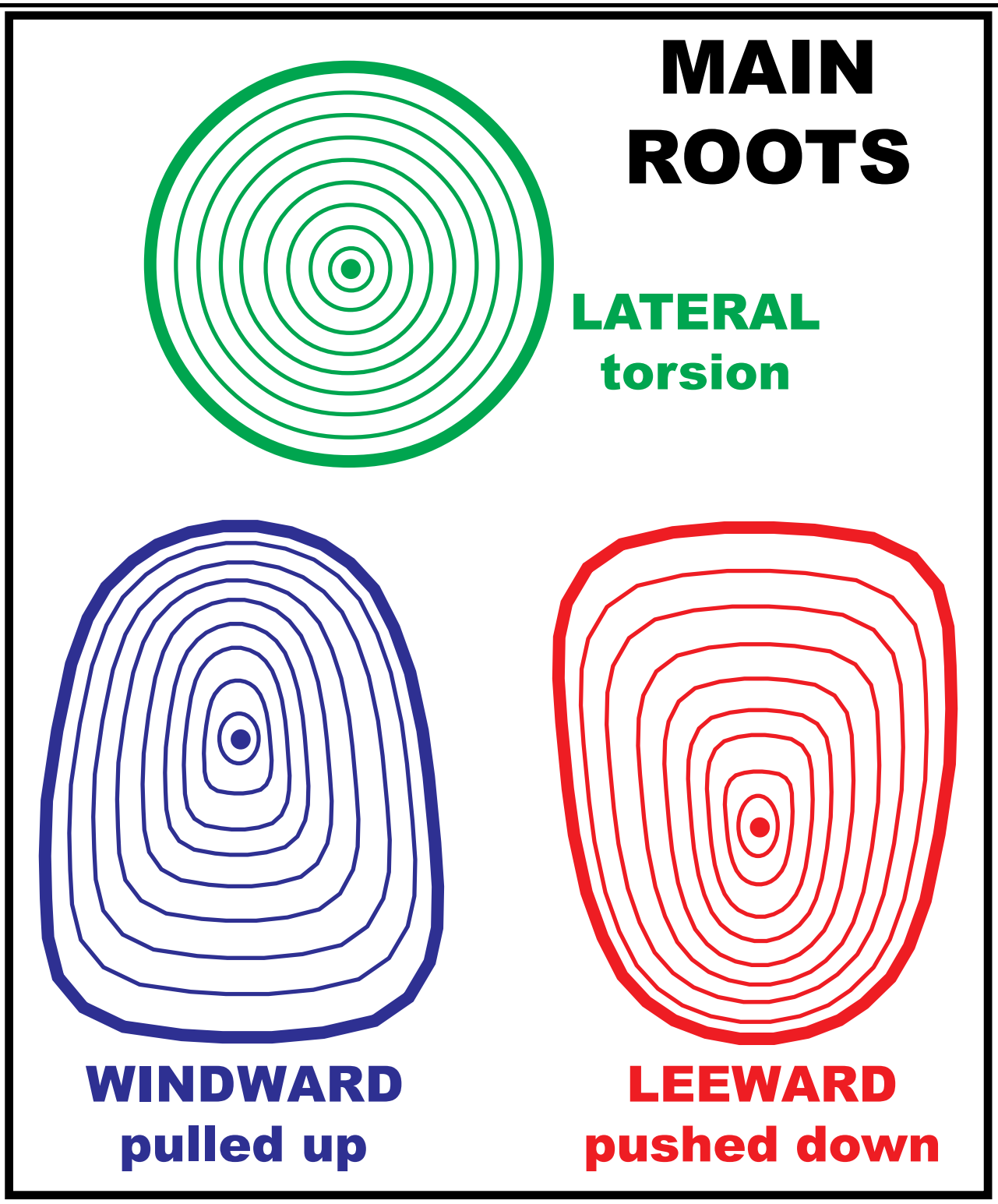

Figure 29: Eccentric growth form of structural roots generated around a tree base to resist wind induced loads. (Stubbs et al. 2019)

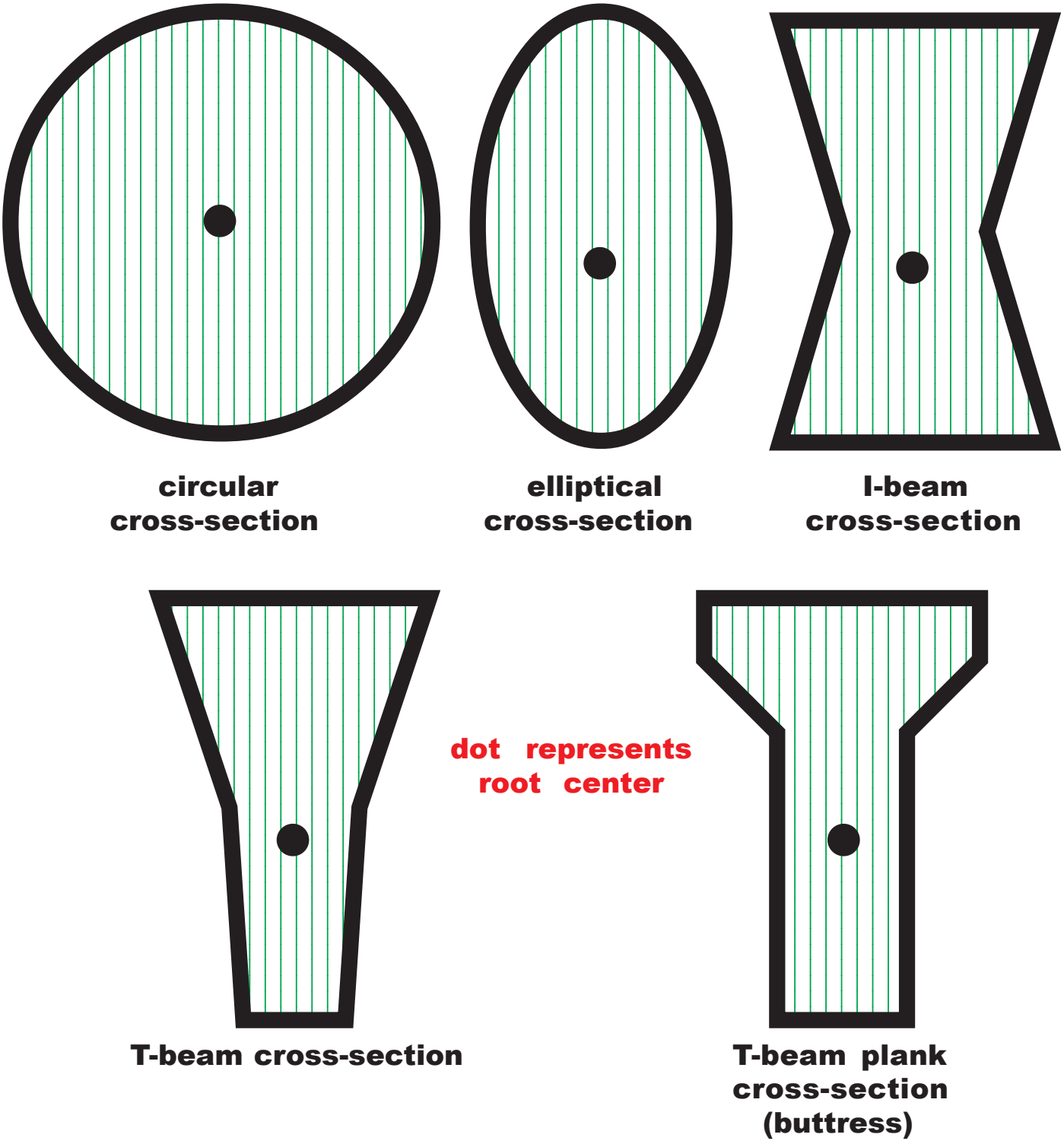

Figure 30: Idealized shapes of root base cross-sections as diameter growth responds to mechanical stress.
(Chiatante et al. 2003; Dilorio et al. 2005;
Nicholl et al. 2006; Nicholl & Ray 1996; Telewski & Moore 2016)

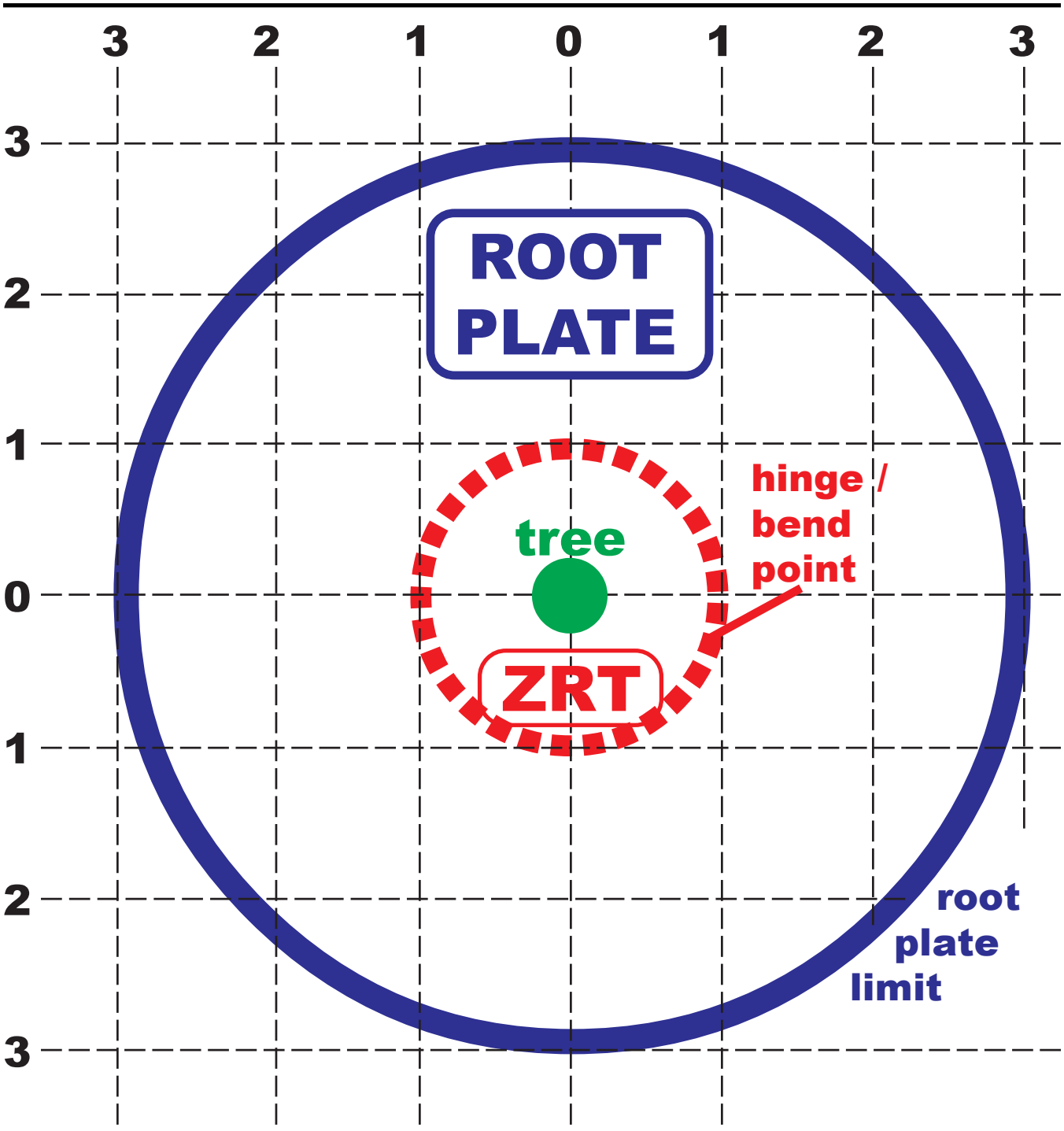

Figure 31: View from above of idealized structural root plate proportions surrounding a tree.
Thick dotted line represents expected leeward hinge point or edge of zone of rapid taper (ZRT).
(Coder 2010; Coder 2018; Danjon et al. 2005; Lundstrom et al. 2007)

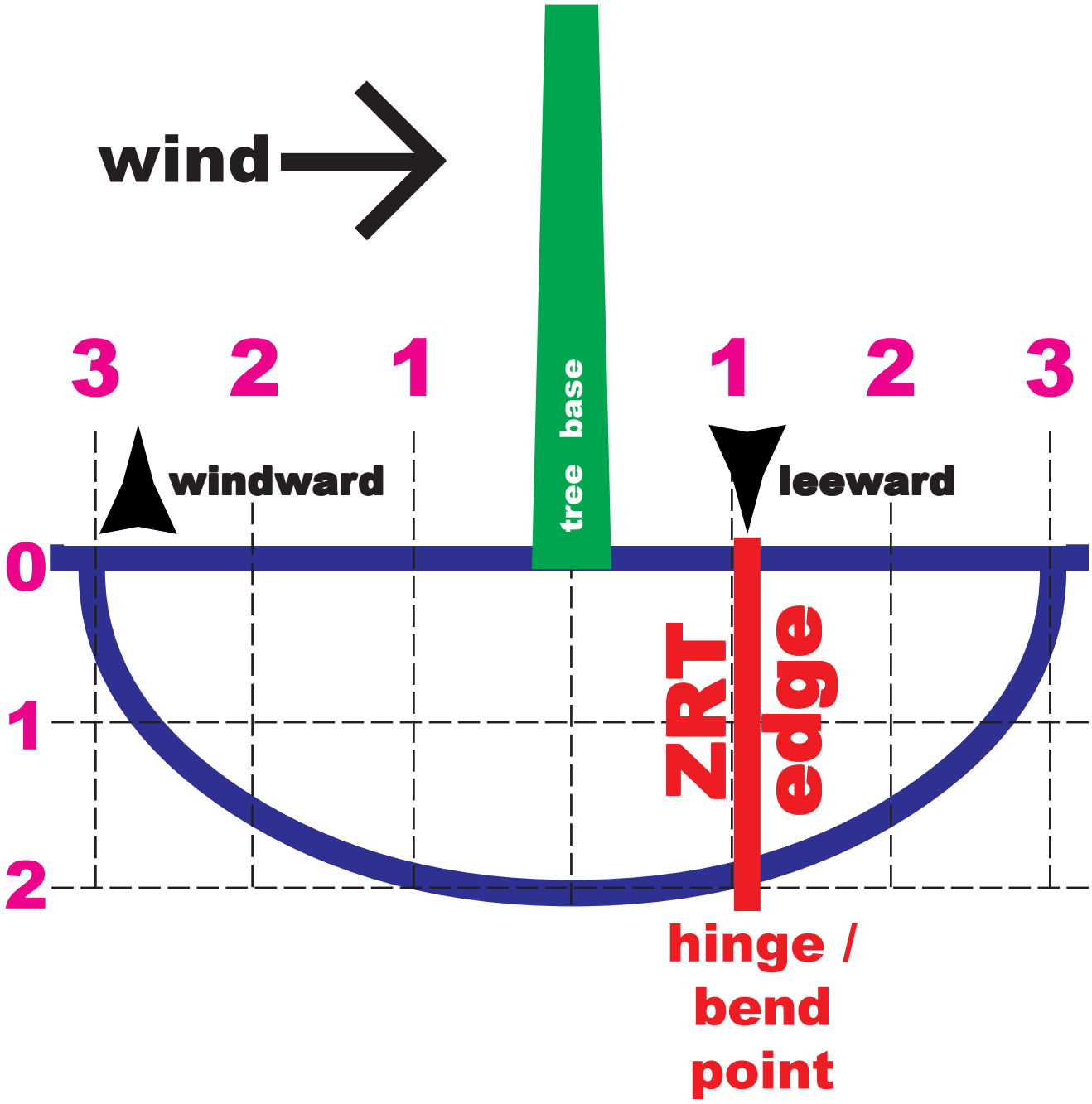

Figure 32: Idealized side view of a wind loaded root plate and edge of ZRT under non-limiting soil conditions. (Coder 2010; Coder 2018; Danjon et al. 2005; Lundstrom et al. 2007)

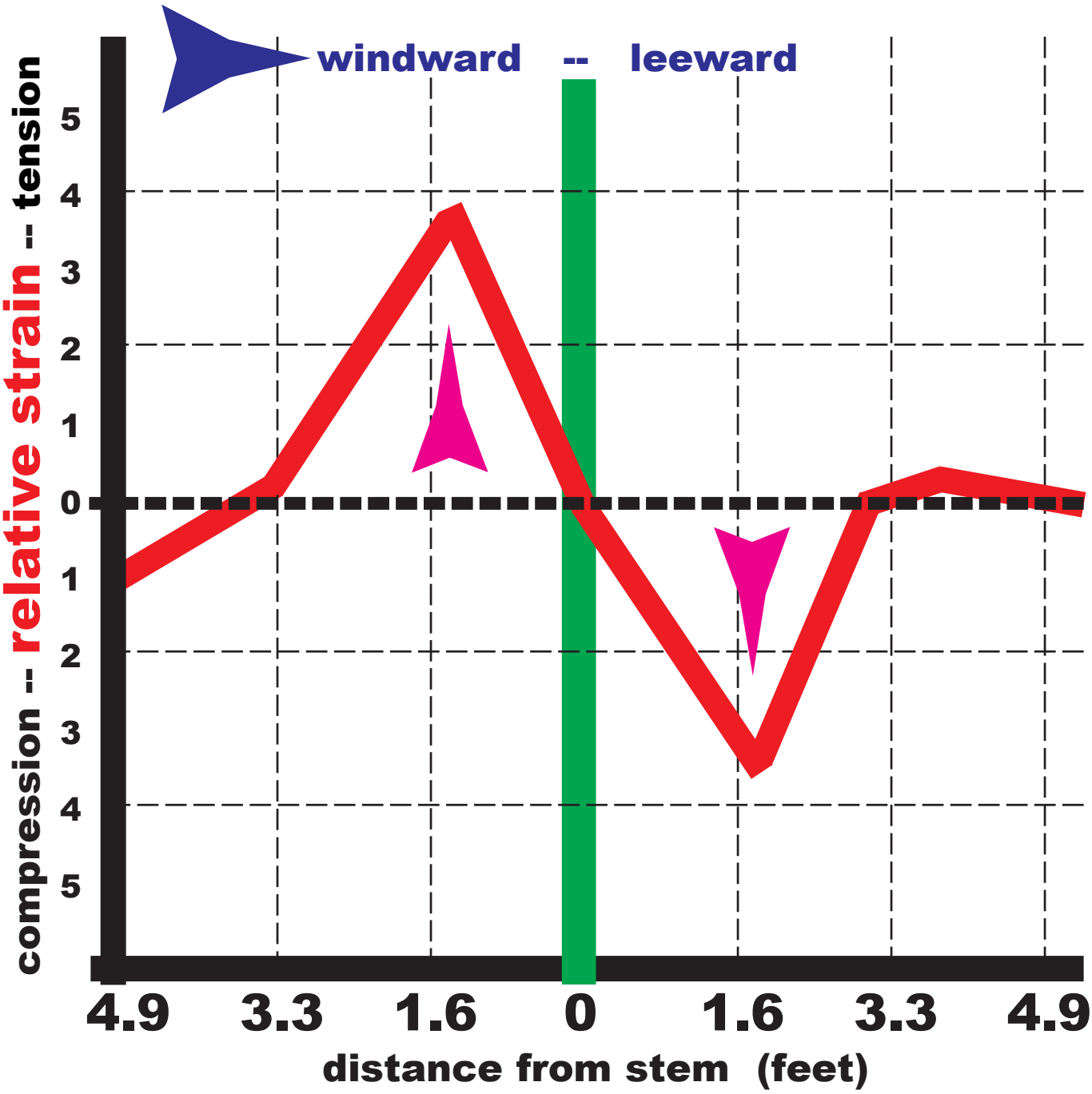

Figure 33: Root strain near tree base under lateral load.
(derived from Sagi et al. 2019)

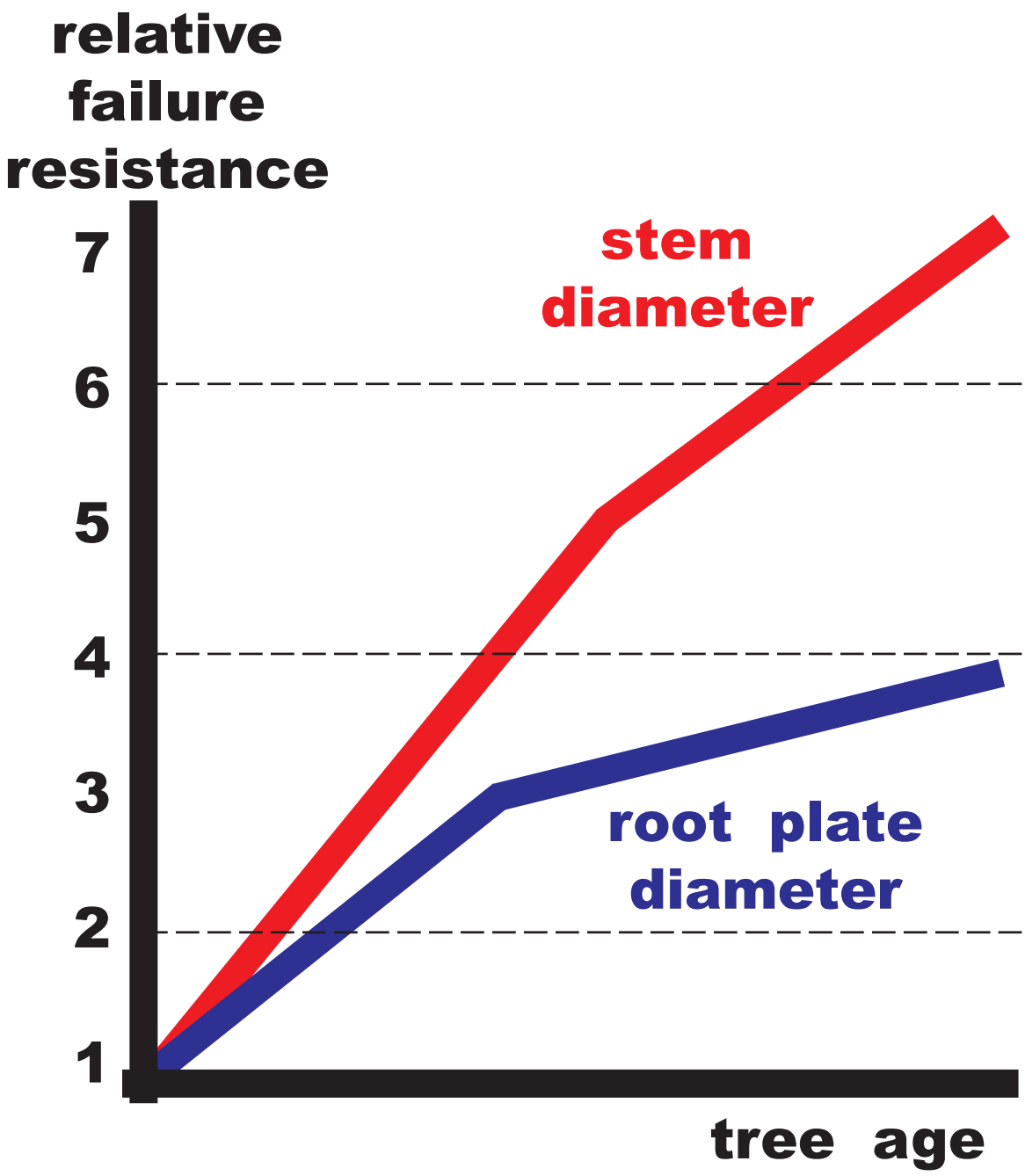

Figure 34: Change in relative resistance to failure of root plate diameter and stem diameter as trees age.
(after Koizumi et al. 2007)